

1 **Inflammatory responses to secondary organic aerosols (SOA) generated from biogenic and**
2 **anthropogenic precursors**

3 *Wing Y. Tuet¹, Yunle Chen², Shierly Fok¹, Julie A. Champion¹, Nga L. Ng^{1,3*}*

4 ¹School of Chemical and Biomolecular Engineering, Georgia Institute of Technology, Atlanta, GA

5 ²School of Materials Science and Engineering, Georgia Institute of Technology, Atlanta, GA

6 ³School of Earth and Atmospheric Sciences, Georgia Institute of Technology, Atlanta, GA

7 **Corresponding Author**

8 *email: ng@chbe.gatech.edu

9 Keywords: reactive oxygen/nitrogen species, inflammatory cytokines, particulate matter, secondary
10 organic aerosol

11 Abstract

12 Cardiopulmonary health implications resulting from exposure to secondary organic
13 aerosols (SOA), which comprise a significant fraction of ambient particulate matter (PM), have
14 received increasing interest in recent years. In this study, alveolar macrophages were exposed to
15 SOA generated from the photooxidation of biogenic and anthropogenic precursors (isoprene, α -
16 pinene, β -caryophyllene, pentadecane, *m*-xylene, and naphthalene) under different formation
17 conditions ($\text{RO}_2 + \text{HO}_2$ vs. $\text{RO}_2 + \text{NO}$ dominant, dry vs. humid). Various cellular responses were
18 measured, including reactive oxygen/nitrogen species (ROS/RNS) production and secreted levels
19 of cytokines, tumor necrosis factor- α (TNF- α) and interleukin-6 (IL-6). SOA precursor identity
20 and formation condition affected all measured responses in a hydrocarbon-specific manner. With
21 the exception of naphthalene SOA, cellular responses followed a trend where TNF- α levels
22 reached a plateau with increasing IL-6 levels. ROS/RNS levels were consistent with relative levels
23 of TNF- α and IL-6, due to their respective inflammatory and anti-inflammatory effects. Exposure
24 to naphthalene SOA, whose aromatic ring-containing products may trigger different cellular
25 pathways, induced higher levels of TNF- α and ROS/RNS than suggested by the trend. Distinct
26 cellular response patterns were identified for hydrocarbons whose photooxidation products shared
27 similar chemical functionalities and structures, which suggests that the chemical structure (carbon
28 chain length and functionalities) of photooxidation products may be important for determining
29 cellular effects. A positive nonlinear correlation was also detected between ROS/RNS levels and
30 previously measured DTT activities for SOA samples. In the context of ambient samples collected
31 during summer and winter in the greater Atlanta area, all laboratory-generated SOA produced
32 similar or higher levels of ROS/RNS and DTT activities. These results suggest that the health

33 effects of SOA are important considerations for understanding the health implications of ambient
34 aerosols.

35 Introduction

36 Particulate matter (PM) exposure is a leading global risk factor for human health (Lim et
37 al., 2012) with numerous studies reporting associations between elevated PM concentrations and
38 increases in cardiopulmonary morbidity and mortality (Li et al., 2008; Pope III and Dockery, 2006;
39 Brunekreef and Holgate, 2002; Dockery et al., 1993; Hoek et al., 2013; Anderson et al., 2011;
40 Pope et al., 2002). A possible mechanism for PM-induced health effects has been suggested by
41 toxicology studies, wherein PM-induced oxidant production, including reactive oxygen and
42 nitrogen species (ROS/RNS), initiates inflammatory cascades thus resulting in oxidative stress and
43 cellular damage (Li et al., 2003a; Tao et al., 2003; Castro and Freeman, 2001; Gurgueira et al.,
44 2002; Wiseman and Halliwell, 1996; Hensley et al., 2000). Furthermore, prolonged stimulation of
45 these inflammatory cascades may lead to chronic inflammation, for which there is a recognized
46 link to cancer (Philip et al., 2004). Together, these findings suggest that a possible relationship
47 exists between PM exposure and observed health effects.

48 Various assays have been developed to study PM-induced oxidant production, including
49 cell-free chemical assays that measure the oxidative potential of PM samples (Kumagai et al.,
50 2002; Cho et al., 2005; Fang et al., 2015b) as well as cellular assays that measure intracellular
51 ROS/RNS produced as a result of PM exposure (Landreman et al., 2008; Tuet et al., 2016). Cell-
52 free assays simulate biologically relevant redox reactions using an antioxidant species (e.g.
53 dithiothreitol, DTT; ascorbic acid, AA). The antioxidant is oxidized via electron transfer reactions
54 catalyzed by redox-active species in the PM sample and its rate of decay serves as a measure of

55 the concentration of redox-active species present (Fang et al., 2015b). On the other hand, cellular
56 assays utilize a fluorescent probe (e.g. carboxy-H₂DCFDA) that reacts with ROS/RNS and the
57 measured fluorescence is proportional to the concentration of ROS/RNS produced as a result of
58 PM exposure (Landreman et al., 2008; Tuet et al., 2016). Both types of assays have been utilized
59 extensively to characterize a variety of PM samples and identify sources that may be detrimental
60 to health (Verma et al., 2015a; Saffari et al., 2015; Fang et al., 2015a; Bates et al., 2015; Li et al.,
61 2003b; Tuet et al., 2016). In particular, numerous studies suggest that organic carbon constituents,
62 especially humic-like substances (HULIS) and oxygenated polycyclic aromatic hydrocarbons (PAH),
63 may contribute significantly to PM-induced oxidant production (Li et al., 2003b; Kleinman et al.,
64 2005; Hamad et al., 2015; Verma et al., 2015b; Lin and Yu, 2011). Furthermore, recent
65 measurements of ROS/RNS production and DTT activity using ambient samples collected in
66 summer and winter around the greater Atlanta area showed that there is a significant correlation
67 between summertime organic species and intracellular ROS/RNS production, suggesting a
68 possible role for secondary organic aerosols (SOA) (Tuet et al., 2016). The same study also
69 reported a significant correlation between ROS/RNS production and DTT activity for summer
70 samples, while a relatively flat ROS/RNS response was observed for winter samples spanning a
71 similar DTT activity range (Tuet et al., 2016). These results highlight a need to consider multiple
72 endpoints as a simple correlation may not exist between different endpoints, especially cellular
73 responses that may result from complicated response networks.

74 Despite these findings, there are still many gaps in knowledge regarding PM-induced
75 health effects. The current work will focus on the relative toxicities of different SOA systems, as
76 field studies have repeatedly shown that SOA often dominate over primary aerosols (e.g., PM
77 emitted directly from combustion engines) even in urban environments (Zhang et al., 2007;

78 Jimenez et al., 2009; Ng et al., 2010). Furthermore, in recent years, there have been an increasing
79 number of studies on the health effects of SOA formed from the oxidation of emitted hydrocarbons,
80 demonstrating their potential contribution to PM-induced health effects (McWhinney et al., 2013;
81 Rattanavaraha et al., 2011; Kramer et al., 2016; Lund et al., 2013; McDonald et al., 2010;
82 McDonald et al., 2012; Baltensperger et al., 2008; Arashiro et al., 2016; Platt et al., 2014;
83 Gallimore et al., 2017). However, the cellular exposure studies involving SOA focused on SOA
84 formed from a single precursor and included different measures of response (e.g. ROS/RNS,
85 inflammatory biomarkers, gene expression, etc.) (Arashiro et al., 2016; Lund et al., 2013;
86 McDonald et al., 2010; McDonald et al., 2012; Baltensperger et al., 2008; Lin et al., 2017). As a
87 result, there is a lack of understanding in terms of the relative toxicity of individual SOA systems.
88 Recently, Tuet et al. (2017) systematically investigated the DTT activities of SOA formed from
89 different biogenic and anthropogenic precursors and demonstrated that intrinsic DTT activities
90 were highly dependent on SOA precursor identity, with naphthalene SOA having the highest DTT
91 activity. As a result, a systematic study on the cellular responses induced by these SOA systems
92 may provide similar insights. Furthermore, cellular responses may complement these previously
93 measured DTT activities to elucidate a more complete picture of the health effects of PM.

94 In the present study, alveolar macrophages were exposed to SOA generated under different
95 formation conditions from various SOA precursors. Cellular responses induced by SOA exposure
96 were measured, including intracellular ROS/RNS production and levels of tumor necrosis factor-
97 α (TNF- α) and interleukin-6 (IL-6). Intracellular ROS/RNS production serves as a general
98 indicator of oxidative stress, whereas TNF- α and IL-6 are pro-inflammatory cytokines indicative
99 of the inflammatory response (Henkler et al., 2010; Kishimoto, 2003; Wang et al., 2003). TNF- α
100 is a hallmark biomarker involved in triggering a number of cellular signaling cascades. More

101 specifically, TNF- α is involved in the activation of NF κ B, which regulates the expression of a
102 variety of genes involved in inflammation and cell death, and the activation of protein kinases,
103 which regulate various signaling cascades (Witkamp and Monshouwer, 2000). IL-6 has both pro-
104 and anti-inflammatory effects, and may directly inhibit TNF- α (Kamimura et al., 2004).
105 Furthermore, both cytokines are produced at relatively high levels in MH-S cells, ensuring a high
106 signal-to-noise ratio and thus reliable measurements (Matsunaga et al., 2001; Chen et al., 2007).
107 Precursors were chosen to include major classes of biogenic and anthropogenic compounds known
108 to produce SOA upon atmospheric oxidation (Table S1). The selected biogenic precursors include:
109 isoprene, the most abundant non-methane hydrocarbon (Guenther et al., 2006); α -pinene, a well-
110 studied monoterpene with emissions on the order of global anthropogenic emissions (Guenther et
111 al., 1993; Piccot et al., 1992); and β -caryophyllene, a representative sesquiterpene. Both
112 monoterpenes and sesquiterpenes have been shown to contribute significantly to ambient aerosol
113 (Eddingsaas et al., 2012; Hoffmann et al., 1997; Tasoglou and Pandis, 2015; Goldstein and
114 Galbally, 2007). Similarly, the anthropogenic precursors include: pentadecane, a long-chain
115 alkane; *m*-xylene, a single-ring aromatic; and naphthalene, a poly-aromatic. These compounds are
116 emitted as products of incomplete combustion (Robinson et al., 2007; Jia and Batterman, 2010;
117 Bruns et al., 2016) and have considerable SOA yields (Chan et al., 2009; Ng et al., 2007b; Lambe
118 et al., 2011). In addition to precursor identity, the effects of humidity (dry vs. humid) and NO_x
119 levels (different predominant peroxy radical (RO₂) fates, RO₂ + HO₂ vs. RO₂ + NO) on SOA
120 cellular inflammatory responses were investigated, as different formation conditions have been
121 shown to affect aerosol chemical composition and mass loading, which could in turn result in a
122 different cellular response (Chhabra et al., 2010; Chhabra et al., 2011; Eddingsaas et al., 2012; Ng
123 et al., 2007b; Loza et al., 2014; Ng et al., 2007a; Chan et al., 2009; Boyd et al., 2015). Finally,

124 correlations between bulk aerosol composition, specifically elemental ratios, and cellular
125 inflammatory responses were investigated to determine whether there is a link between different
126 inflammatory responses and aerosol composition.

127 **Methods**

128 **Alveolar macrophage cell line.** Exposures were conducted using immortalized murine
129 alveolar macrophages (MH-S, ATCC®CRL-2019™) as they are the first line of defense against
130 environmental insults (Oberdörster, 1993; Oberdörster et al., 1992). The particular cell line also
131 retains many properties of primary alveolar macrophages, including phagocytosis as well as the
132 production of ROS/RNS and cytokines (Sankaran and Herscowitz, 1995; Mbawuike and
133 Herscowitz, 1989). MH-S cells were cultured in RPMI-1640 media supplemented with 10% fetal
134 bovine serum (FBS, Quality Biological, InC.), 1% penicillin-streptomycin, and 50 μ M β -
135 mercaptoethanol (BME) at 37°C and humid air containing 5% CO₂. For exposure experiments,
136 MH-S cells were seeded at a density of 2 x 10⁴ cells well⁻¹ onto 96-well plates pre-treated with
137 10% FBS in phosphate buffered saline (PBS, Cellgro). For seeding and all assay procedures
138 thereon, FBS-supplemented cell culture media without BME addition was used as BME is a
139 reducing agent that may interfere with inflammatory measurements.

140 **Chamber experiments.** SOA formed from the photooxidation of biogenic and
141 anthropogenic precursors were generated in the Georgia Tech Environmental Chamber (GTEC)
142 facility. Details of the facility have been described elsewhere (Boyd et al., 2015). Briefly, the
143 chamber facility consists of two 12 m³ Teflon chambers suspended within a 21 x 12 ft temperature-
144 controlled enclosure. Black lights and natural sunlight fluorescent lamps surround the chambers,
145 and multiple sampling ports allow for injection of reagents, as well as gas- and aerosol-phase

146 measurements. Gas-phase O₃, NO₂, and NO_x concentrations were monitored using an O₃ analyzer
147 (Teledyne T400), a cavity attenuated phase shift (CAPS) NO₂ monitor (Aerodyne), and a
148 chemiluminescence NO_x monitor (Teledyne 200EU) respectively, while hydrocarbon decay was
149 monitored using a gas chromatography-flame ionization detector (GC-FID, Agilent 7890A).
150 Hydrocarbon decay was also used to estimate hydroxyl radical (OH) concentrations. For aerosol-
151 phase measurements, a Scanning Mobility Particle Sizer (SMPS, TSI) was used to measure aerosol
152 volume concentrations and distributions, while a High Resolution Time-of-Flight Aerosol Mass
153 Spectrometer (HR-ToF-AMS, Aerodyne; henceforth referred to as the AMS) was used to
154 determine bulk aerosol composition (DeCarlo et al., 2006). AMS data was analyzed using the data
155 analysis toolkit SQUIRREL (v. 1.57) and PIKA (v. 1.16G). Elemental ratios, including O:C, H:C,
156 and N:C, were obtained using the method outlined by Canagaratna et al. (2015) and used to
157 calculate the average carbon oxidation state (\overline{OS}_c) (Kroll et al., 2011). Temperature and relative
158 humidity (RH) were also monitored using a hydro-thermometer (Vaisala HMP110).

159 Experiments were designed to probe the effects of humidity, RO₂ fate, and precursor
160 identity on cellular inflammatory responses induced by different SOA formed under these
161 conditions (Table 1). All chamber experiments were performed at \sim 25 °C under dry (RH < 5%) or
162 humid (RH \sim 45%) conditions. Chambers were flushed with pure air (generated from AADCO,
163 747-14) for \sim 24 hrs prior to each experiment. During this time, chambers were also humidified for
164 humid experiments by means of a bubbler filled with deionized (DI) water. Seed aerosol was
165 injected by atomizing a 15 mM (NH₄)₂SO₄ seed solution (Sigma Aldrich) to obtain a seed
166 concentration of \sim 20 μ g m⁻³. It should be noted that experimental conditions deviate for experiment
167 7 (isoprene SOA under RO₂ + HO₂ dominant, “humid” conditions) due to low SOA mass yields.
168 For this experiment, an acidic seed solution (8 mM MgSO₄ and 16 mM H₂SO₄) and a dry chamber

169 were used to promote SOA formation via the isoprene epoxydiol (IEPOX) uptake pathway. This
170 pathway has been shown to contribute significantly to ambient OA and has a higher SOA mass
171 yield compared to the IEPOX + OH pathway (Surratt et al., 2010; Lin et al., 2012; Xu et al., 2015).

172 SOA precursor was then introduced by injecting a known amount of hydrocarbon solution
173 [isoprene, 99%; α -pinene, \geq 99%; β -caryophyllene, $>$ 98.5%; pentadecane, \geq 99%; *m*-xylene, \geq
174 99%; naphthalene, 99% (Sigma Aldrich)] into a glass injection bulb and passing pure air over the
175 solution until it fully evaporated. For pentadecane and β -caryophyllene, the glass bulb was also
176 heated gently during hydrocarbon injection to ensure full evaporation (Tasoglou and Pandis,
177 2015). Naphthalene was injected by passing pure air over solid naphthalene flakes as described in
178 previous studies (Chan et al., 2009). OH precursor was then introduced via injection of hydrogen
179 peroxide (H_2O_2) for $\text{RO}_2 + \text{HO}_2$ experiments or nitrous acid (HONO) for $\text{RO}_2 + \text{NO}$ experiments.
180 For H_2O_2 , a 50% aqueous solution (Sigma Aldrich) was injected using the same method described
181 for hydrocarbon injection to achieve an H_2O_2 concentration of 3 ppm. This amount yielded OH
182 concentrations on the order of 10^6 molec cm^{-3} . For HONO injections, HONO was first prepared
183 by adding 10 mL of 1%wt aqueous NaNO_2 (VWR International) dropwise into 20 mL of 10%wt
184 H_2SO_4 (VWR International) in a glass bulb. Zero air was then passed over the solution to introduce
185 HONO into the chamber (Chan et al., 2009; Kroll et al., 2005). Photolysis of HONO yielded OH
186 concentrations on the order of 10^7 molec cm^{-3} . NO and NO_2 were also formed as byproducts of
187 HONO synthesis. Once all the H_2O_2 evaporated ($\text{RO}_2 + \text{HO}_2$ experiments) or NO_x concentrations
188 stabilized ($\text{RO}_2 + \text{NO}$ experiments), the UV lights were turned on to initiate photooxidation.

189 **Aerosol collection and extraction.** Aerosol samples were collected onto 47 mm TeflonTM
190 filters (0.45 μm pore size, Pall Laboratory). The total mass collected onto each filter was
191 determined by integrating the SMPS time-dependent volume concentration over the filter

192 collection period and multiplying by the total volume of air collected. SMPS volume
193 concentrations were converted to mass concentrations by assuming a density of 1 g cm⁻³ to
194 facilitate comparison between studies. To account for potential H₂O₂ or HONO uptake,
195 background filters were also collected. These filters were collected when only seed particles and
196 OH precursor (H₂O₂ or HONO) were injected into the chamber under otherwise identical
197 experimental conditions. All collected samples were placed in sterile petri dishes, sealed with
198 Parafilm M®, and stored at -20 °C until extraction and analysis (Fang et al., 2015b). Collected
199 particles were extracted following the procedure outlined in Fang et al. (2015a) with modifications
200 for cellular exposure. Briefly, filter samples were submerged in cell culture media (RPMI-1640)
201 and sonicated for two 30 min intervals (1 hr total) using an Ultrasonic Cleanser (VWR
202 International). In between sonication intervals, the water was replaced to reduce bath temperature.
203 After the final sonication interval, sample extracts were filtered using 0.45 µm PTFE syringe filters
204 (Fisherbrand™) to remove any insoluble material and supplemented with 10% FBS (Fang et al.,
205 2015b).

206 **Intracellular ROS/RNS measurement.** ROS/RNS were detected using the assay
207 optimized in Tuet et al. (2016). Briefly, the assay consists of five major steps: (1) pre-treatment of
208 96-well plates to ensure a uniform cell density, (2) seeding of cells onto pre-treated wells at 2 x
209 10⁴ cells well⁻¹, (3) incubation with ROS/RNS probe (carboxy-H₂DCFDA, Molecular Probes C-
210 400) diluted to a final concentration of 10 µM, (4) exposure of probe-treated cells to samples and
211 controls for 24 hrs, and (5) detection of ROS/RNS using a microplate reader (BioTek Synergy H4,
212 ex/em: 485/525 nm). Positive controls included bacterial cell wall component lipopolysaccharide
213 (LPS, 1 µg mL⁻¹), H₂O₂ (100 µM), and reference filter extract (10 filter punches mL⁻¹, 1 per filter
214 sample, from various ambient filters collected at the Georgia Tech site, while negative controls

215 included blank filter extract (2 punches mL^{-1}) and control cells (probe-treated cells exposed to
216 media only, no stimulants).

217 A previous study on the ROS/RNS produced induced by exposure to ambient PM samples
218 found that ROS/RNS production was highly dose-dependent and could therefore not be
219 represented by measurements taken at a single dose (Tuet et al., 2016). Here, we utilize the dose-
220 response curve approach described in Tuet et al. (2016). For each aerosol sample, ROS/RNS
221 production was measured over ten dilutions and expressed as a fold increase in fluorescence over
222 control cells. A representative dose-response curve is shown in Fig. 1. For comparisons to other
223 inflammatory endpoints and chemical composition, ROS/RNS production was represented using
224 the area under the dose-response curve (AUC), as AUC has been shown to be the most robust
225 metric for comparing PM samples (Tuet et al., 2016).

226 **Cytokine measurement.** Secreted levels of TNF- α and IL-6 were measured post-exposure
227 (24 hrs) using enzyme-linked immunosorbent assay (ELISA) kits following manufacturer's
228 specifications (ThermoFisher). This time point was chosen to enable comparison with ROS/RNS
229 levels (also measured at 24 hrs, optimized in Tuet et al. (2016)) and to ensure a high signal for
230 both cytokines. Previous literature have shown that TNF- α and IL-6 production peak around 4 and
231 24 hrs, respectively (Haddad, 2001). However, while TNF- α production peaks earlier, the signal
232 at 24 hrs is well above the detection limit of the assay, and previous studies have utilized this time
233 point to measure both cytokines (Haddad, 2001; Matsunaga et al., 2001). Nonetheless, it should
234 be noted that these measurements represent a single time point in the cellular response. All
235 measurements were carried out using undiluted cell culture supernatant. For each aerosol sample,
236 TNF- α and IL-6 were measured over seven dilutions and represented as a fold increase over
237 control. Similarly, the AUC was used to represent each endpoint for comparison purposes.

238 **Cellular metabolic activity.** The MTT (3-(4,5-dimethylthiazol-2-yl)-2,5-
239 diphenyltetrazolium bromide) assay (Biotium) was used to assess cellular metabolic activity.
240 Briefly, supernatants containing sample extracts were removed after the exposure period and
241 replaced with media containing MTT. Cells were then returned to the incubator for 4 hrs, during
242 which the tetrazolium dye was reduced by cellular NAD(P)H-dependent oxidoreductases to
243 produce an insoluble purple salt (formazan). Dimethyl sulfoxide was then used to solubilize the
244 salt and the absorbance at 570 nm was determined using a microplate reader (BioTek Synergy H4).

245 **Statistical analysis.** Linear regressions between bulk aerosol composition and cellular
246 inflammatory responses were evaluated using Pearson's correlation coefficient, and the
247 significance of each correlation coefficient was determined using multiple imputation, which
248 calculated the total variance associated with the slope of each regression. Details of this method
249 are described in Pan and Shimizu (2009). Briefly, response parameters (i.e. AUCs for each
250 endpoint) were assumed to follow a normal distribution. Ten “estimates” were obtained for each
251 response using the average and standard deviation determined from the dose-response curve fit.
252 These estimates were then plotted against bulk aerosol composition (e.g. O:C, H:C, and N:C) to
253 obtain ten fits, and the slopes and variances generated from these fits were used to calculate the
254 between and within variance. Finally, a Student's *t*-test was used to calculate and evaluate the
255 associated *p*-values using a 95% confidence interval.

256 Results and Discussion

257 **Effect of SOA precursor and formation condition on SOA inflammatory response.** To
258 investigate whether SOA formed from different precursors elicited different inflammatory
259 responses, levels of ROS/RNS, TNF- α , and IL-6 were measured after exposing alveolar

260 macrophages to SOA generated from six VOCs generated under three formation conditions (Table
261 1). The AUC per mass of SOA (µg) in the extract for ROS/RNS, TNF- α and IL-6 are shown in
262 Fig. 2, shaped by SOA formation condition. It should be noted that all responses were normalized
263 to probe-treated control cells to account for differences between endogenous levels of ROS/RNS
264 produced in cells (Henkler et al., 2010). Uncertainties associated with AUC were determined by
265 averaging the AUCs obtained by fitting dose-response data with each point removed
266 systematically, following the methodology described in Tuet et al. (2016). ROS/RNS production
267 was also measured for background filters and found to be within the uncertainty of control cells,
268 indicating that there was no evidence for significant H₂O₂ or HONO uptake onto seed particles
269 (Fig. S1). Furthermore, exposure to filter extract did not result in decreases in metabolic activity
270 as measured by the MTT assay for all SOA systems investigated (Fig. S2). Since results from MTT
271 may represent the number of viable cells present, changes in inflammatory endpoints did not likely
272 result from changes in the number of cells exposed (i.e. decreases in response cannot be attributed
273 to cell death).

274 For all inflammatory responses measured (levels of ROS/RNS, TNF- α , and IL-6), SOA
275 precursor identity and formation condition influenced the level of response, as demonstrated by
276 the range of values obtained from different SOA precursors and different formation conditions
277 (Fig. 2). Despite having a clear effect, no obvious trends were observed for each variable (precursor
278 or formation condition) on individual responses. This is in contrast to that observed for the
279 oxidative potential as measured by DTT (OP^{WS-DTT}) for these samples, where only precursor
280 identity influenced OP^{WS-DTT} substantially (Tuet et al., 2017). However, this may not be surprising
281 as DTT is a chemical assay, which only accounts for the potential of species to participate in redox
282 reactions (Cho et al., 2005), whereas cellular assays account for many complicated cellular events

283 involved in intricate positive and negative feedback loops. Due to the considerably different
284 classes of compounds chosen as SOA precursors, aerosol compositional changes between different
285 precursors were generally larger than those between different formation conditions of the same
286 precursor (see Fig. 3a) (Tuet et al., 2017). DTT may only be sensitive to larger differences arising
287 from different precursors, whereas cellular assays could also be sensitive to differences between
288 different formation conditions and chemical composition of the same precursor. Moreover, while
289 Tuet et al. (2017) showed that the intrinsic OP^{WS-DTT} spanned a wide range, with isoprene and
290 naphthalene SOA generating the lowest and highest OP^{WS-DTT} , these bounds were less clear for
291 cellular responses. While isoprene and naphthalene SOA still generated the lowest and highest
292 inflammatory responses in general, a few exceptions exist (e.g. ROS/RNS levels induced by
293 pentadecane SOA formed under dry, $RO_2 + HO_2$ dominant conditions, Fig. 2).

294 Though no apparent trends in individual inflammatory responses were observed as a
295 function of SOA precursor identity or formation condition, several patterns among all three
296 inflammatory responses were observed for SOA precursors whose products share similar chemical
297 structures (i.e., similar carbon chain length and functionalities). Exposure to isoprene SOA induced
298 the lowest levels of TNF- α and IL-6 among the aerosol systems studied (Fig. 2). Furthermore,
299 isoprene SOA generated from different pathways (i.e. photooxidation under different RO_2 fates
300 and reactive uptake of IEPOX) (Surratt et al., 2010; Xu et al., 2014; Chan et al., 2010) produced
301 similar responses for each inflammatory endpoint. These results suggest that different isoprene
302 SOA products (Surratt et al., 2010; Xu et al., 2014; Chan et al., 2010) may induce similarly low
303 inflammatory responses and are consistent with the intrinsic OP^{WS-DTT} obtained for these SOA
304 samples, where isoprene SOA generated the lowest OP^{WS-DTT} of all SOA systems studied and the
305 OP^{WS-DTT} was similar for all SOA formation conditions explored (Tuet et al., 2017). This finding

306 is in contrast to a previous study by Lin et al. (2016), where methacrylic acid epoxide (MAE)-
307 derived SOA was found to be substantially more potent than IEPOX-derived SOA. However,
308 while exposure to MAE-derived SOA induced the upregulation of a larger number of oxidative
309 stress response genes than IEPOX-derived SOA, the fold change of several genes reported in Lin
310 et al. (2016) are actually similar (e.g., *ALOX12*, *NQO1*). Several of these genes directly affect the
311 production of inflammatory cytokines measured in this study. For instance, studies have observed
312 that arachidonate 12-lipoxygenase (*ALOX12*) products induce the production of both TNF- α and
313 IL-6 in macrophages (Wen et al., 2007). As such, a similar response level regardless of SOA
314 formation condition may be observed depending on the biological endpoints measured. Thus, it is
315 possible that the inflammatory cytokines measured in this study are involved in pathways
316 concerning those genes, resulting in a similar response level regardless of SOA formation
317 condition.

318 Similarly, exposure to SOA generated from the photooxidation of α -pinene and *m*-xylene
319 resulted in similar inflammatory responses for all three formation conditions (Fig. 2). These
320 cellular assay results are consistent with results from the DTT assay where the OP^{WS-DTT} was not
321 significantly different between SOA formed under different formation conditions (Tuet et al.,
322 2017). Response levels induced by these two SOA systems are also similar across all three
323 inflammatory measurements investigated (Fig. 2). This suggests that products from both
324 precursors may induce similar cellular pathways resulting in the production of similar levels of
325 inflammatory markers. Indeed, there are several similarities between products formed from the
326 photooxidation of α -pinene and *m*-xylene. For instance, a large portion of α -pinene and *m*-xylene
327 oxidation products under both RO₂ + HO₂ and RO₂ + NO pathways are ring-breaking products
328 with a similar carbon chain length (Eddingsaas et al., 2012; Vivanco and Santiago, 2010; Jenkin

329 et al., 2003). As a result of this similarity, products from both SOA systems may interact with the
330 same cellular targets and induce similar cellular pathways, resulting in a similar response
331 regardless of precursor identity and formation condition. These observations further imply that the
332 chemical structures (e.g., carbon chain lengths and functionalities) of oxidation products may be
333 important regardless of PM source/precursor.

334 A different pattern was observed for β -caryophyllene and pentadecane SOA, where the IL-
335 6 response spanned a much larger range than ROS/RNS and TNF- α (Fig. 2). This is in contrast to
336 the trends observed for the OP^{WS-DTT} for β -caryophyllene and pentadecane SOA, where OP^{WS-DTT}
337 was similar regardless of formation condition (Tuet et al., 2017). This suggests that there are
338 differences between organic peroxides and organic nitrates formed from certain precursors that
339 influence cellular responses, but are not captured by redox potential measurements. Less is known
340 about the effects of humidity on SOA formation and chemical composition for all SOA systems
341 investigated, as most laboratory chamber studies in literature have been conducted under dry
342 conditions. Specifically here, very high levels of IL-6 were observed post-exposure to pentadecane
343 SOA formed under humid conditions. Prior studies reported opposing findings with some showing
344 a significant effect of water on aerosol formation and chemical composition (Nguyen et al., 2011;
345 Wong et al., 2015; Healy et al., 2009; Stirnweis et al., 2016), while others found little influence
346 (Edney et al., 2000; Boyd et al., 2015; Cocker III et al., 2001). It is clear that humidity effects are
347 highly hydrocarbon-dependent and further studies into the specific products formed under humid
348 conditions are required to understand how these differences in chemical composition may translate
349 to different cellular endpoints. Nonetheless, the known products formed from the photooxidation
350 of these hydrocarbons may provide some insight into the inflammatory responses observed. While
351 there are no prior studies involving pentadecane oxidation products, it is expected that the

352 oxidation products will be similar to those reported in the oxidation of dodecane (i.e. same
353 functionalities with a longer carbon chain) (Loza et al., 2014). It is therefore likely that pentadecane
354 oxidation products resemble long chain fatty acids and could potentially insert into the cell
355 membrane (Loza et al., 2014), as previous studies have shown that fatty acids can feasibly insert
356 into the cell membrane bilayer (Khmelinskaia et al., 2014; Cerezo et al., 2011). This insertion
357 could potentially affect membrane fluidity, which is known to affect cell function substantially
358 although the specific effect depends strongly on the particular modification and cell type of interest
359 (Baritaki et al., 2007; Spector and Yorek, 1985). In some cases, these alterations lead to the
360 induction of apoptosis, which involves pathways leading to the production of TNF- α (Baritaki et
361 al., 2007; Wang et al., 2003). TNF- α can then induce the production of IL-6, which once produced
362 can also inhibit the production of TNF- α in a feedback loop (Kishimoto, 2003; Wang et al., 2003).
363 These cellular events are consistent with the observed inflammatory response induced by
364 pentadecane SOA exposure, where there is a high IL-6 response and a lower TNF- α response. The
365 low ROS/RNS response observed is also in line with these cellular events, as IL-6 exhibits anti-
366 inflammatory functions, which can neutralize ROS/RNS production. These responses are less
367 pronounced for β -caryophyllene aerosol, which may be due to the shorter carbon chain observed
368 in known products (Chan et al., 2011). While β -caryophyllene and pentadecane are both C15
369 precursors, β -caryophyllene is a bicyclic compound and many SOA products retain the 4-
370 membered ring, resulting in a shorter carbon backbone (Chan et al., 2011). As a result, fewer
371 products may insert into the cell membrane, leading to a lesser response compared to pentadecane
372 SOA exposure. These observations, particularly those for pentadecane SOA, suggest that aerosols
373 from meat cooking may have health implications, as fatty acids comprise a majority of these
374 aerosols (Mohr et al., 2009; Rogge et al., 1991).

375 Naphthalene exhibits a different, more distinct pattern compared to the rest of the SOA
376 systems investigated, with a large range observed for both TNF- α and IL-6 under different
377 formation conditions (Fig. 2). Higher levels of ROS/RNS were also observed as a result of
378 exposure to naphthalene aerosol irrespective of SOA formation condition. Similarly, the OP^{WS-DTT}
379 of naphthalene SOA previously measured by Tuet et al. (2017) was an outlier among all SOA
380 systems investigated, as the measured OP^{WS-DTT} was at least twice that of the next highest SOA
381 system. These observations are consistent with the formation of specific SOA products such as
382 naphthoquinones, which are known to induce redox-cycling in cells and are formed under both
383 RO₂ + HO₂ and RO₂ + NO pathways (Henkler et al., 2010; Kautzman et al., 2010). Consequently,
384 aerosol generated from naphthalene may induce higher levels of inflammatory responses than
385 other SOA due to this process (Henkler et al., 2010; Lorentzen et al., 1979). However, as shown
386 by the high levels of IL-6, exposure to naphthalene SOA may also induce anti-inflammatory
387 pathways not captured by OP^{WS-DTT} measurements. Moreover, a clear increasing trend is apparent
388 for TNF- α and IL-6 produced upon naphthalene SOA exposure, with a higher level of both
389 cytokines observed for aerosol formed under RO₂ + NO dominant and humid conditions.
390 Previously, the effect of different RO₂ fates on SOA OP^{WS-DTT} was attributed to the different
391 products known to form under both pathways (Tuet et al., 2017). The same explanation applies for
392 cellular measurements as SOA products that promote electron transfer reactions with antioxidants
393 can result in redox imbalance as measured by OP^{WS-DTT} and the induction of related cellular
394 pathways such as ROS/RNS and cytokine production (Tuet et al., 2017). Finally, naphthalene SOA
395 induced cellular responses outside of those observed for other aerosol systems, with higher levels
396 of all inflammatory markers than other SOA systems. As shown previously for OP^{WS-DTT},
397 naphthalene may be an outlier due to aromatic ring-containing products, which may then induce

398 different cellular pathways compared to other aerosol systems investigated, the products of which
399 do not contain aromatic rings. Additionally, many known aerosol products formed from the
400 photooxidation of naphthalene have functionalities that resemble those of dinitrophenol, which is
401 known to decouple phosphorylation from electron transfer (Terada, 1990). It is therefore possible
402 that the aromatic functionality present in the majority of naphthalene SOA products results in the
403 involvement of very different cellular pathways, leading to outlier inflammatory endpoint
404 responses. Various products of naphthalene oxidation such as nitroaromatics and polyaromatics
405 are known to have mutagenic properties and may induce the formation of DNA adducts (Baird et
406 al., 2005; Helmig et al., 1992). As such, it is possible that these products may induce health effects
407 via other pathways as well and naphthalene SOA exposure may have effects beyond redox
408 imbalance and oxidative stress.

409 Bulk aerosol elemental ratios (O:C, H:C, and N:C) were determined for each SOA system
410 investigated. Different types of organic aerosol are known to span a wide range of O:C, which may
411 be utilized as an indication of oxidation, and the van Krevelen diagram was used to visualize
412 whether changes in O:C and H:C ratios corresponded to changes in levels of inflammatory
413 response (Fig. 3a, S3) (Chhabra et al., 2011; Lambe et al., 2011; Ng et al., 2010). Changes in the
414 slope within the van Krevelen space provide information on SOA functionalization (Heald et al.,
415 2010; Van Krevelen, 1950; Ng et al., 2011). Beginning from the precursor hydrocarbon, a slope
416 of 0 indicates alcohol group additions, a slope of -1 indicates carbonyl and alcohol additions on
417 separate carbons or carboxylic acid additions, and a slope of -2 indicates ketone or aldehyde
418 additions.

419 As seen in Fig. 3a, the laboratory-generated aerosols span a large range of O:C and H:C
420 ratios. Both SOA formation condition and precursor identity influenced elemental ratios, however,

421 precursor identity generally had a larger effect as evident by the clusters observed for different
422 SOA precursors. Despite these differences in chemical composition, there were no obvious trends
423 between O:C or H:C and any inflammatory endpoint measured. This is similar to that observed for
424 chemical oxidative potential as measured by DTT, where a higher O:C did not correspond to a
425 higher oxidative potential for both laboratory-generated and ambient aerosols (Tuet et al., 2017).
426 This is likely due to the different formation conditions used to generate SOA, which may not be
427 directly comparable. Nevertheless, a significant correlation ($p < 0.05$) was observed between
428 ROS/RNS and \overline{OS}_c (Fig. 3b). This positive correlation is not surprising, as a higher average
429 oxidation state would likely correspond to a better oxidizing agent. Future studies should evaluate
430 the effect of the degree of oxidation for SOA formed from the same SOA precursor under the same
431 formation condition to investigate whether atmospheric aging of aerosol (which typically leads to
432 increases in the degree of oxidation) affects inflammatory responses. Finally, the N:C ratio was
433 also determined for SOA systems formed under conditions that favor the $RO_2 + NO$ pathway (Fig.
434 S4) and were found to span a large range. Similarly, there was no obvious trend between N:C ratios
435 and the inflammatory endpoints measured.

436 **Relationship between inflammatory responses.** To visualize whether there exists a
437 relationship between inflammatory markers measured, levels of TNF- α and IL-6 are shown in Fig.
438 4, sized by ROS/RNS. With the exception of naphthalene SOA, the inflammatory cytokine
439 responses for all aerosol systems investigated follow an exponential curve (Fig. 4, shown in black)
440 where there appears to be a plateau for TNF- α levels. Along this curve, ROS/RNS levels also
441 appear to increase with increasing inflammatory cytokine levels to a certain point, after which
442 ROS/RNS levels decrease. These observations are in line with the interconnected effects of both
443 cytokines. While both TNF- α and IL-6 have pro-inflammatory effects that may lead to the increase

444 of ROS/RNS production, the individual pathways are also involved in many complicated
445 stimulation and inhibition loops and there is extensive cross-talk between both pathways. For
446 instance, TNF- α induces the production of glucocorticoids, which in turn inhibits both TNF- α and
447 IL-6 production (Wang et al., 2003). IL-6 also directly inhibits the production of TNF- α and other
448 cytokines induced as a result of TNF- α (e.g. IL-1) and stimulates pathways that lead to the
449 production of glucocorticoids (Kishimoto, 2003). As a result, increases in IL-6 may be
450 accompanied by decreases in TNF- α , resulting in the observed plateau. Furthermore, ROS/RNS
451 levels may represent a fine balance between anti-inflammatory and pro-inflammatory effects. Both
452 cytokines are involved in the acute phase reaction and can affect ROS/RNS levels via pro-
453 inflammatory pathways. IL-6 also exhibits some anti-inflammatory functions and may thus lower
454 ROS/RNS levels as well. These interconnected pathways could account for the observed parabolic
455 pattern for ROS/RNS production. Exposure to naphthalene SOA resulted in responses outside of
456 those observed for other aerosol systems, likely due to the formation of aromatic ring-retaining
457 products as discussed in the previous section.

458 **Comparison with ambient data.** To evaluate how the oxidative potential and ROS/RNS
459 production of the SOA systems investigated compare in the context of ambient samples, the
460 measurements obtained in this study were plotted with those obtained in our previous study
461 involving ambient samples collected around the greater Atlanta area (Fig. 5) (Tuet et al., 2016).
462 These ambient samples were analyzed using the same methods for determining oxidative potential
463 (DTT assay (Cho et al., 2005; Fang et al., 2015b)) and ROS/RNS production (cellular carboxy-
464 H₂DCFDA assay (Tuet et al., 2016)). Furthermore, the same extraction protocol (water-soluble
465 extract) was followed in both studies (Tuet et al., 2016). Results from both studies are therefore
466 directly comparable. Previously, a significant correlation between ROS/RNS production and

467 oxidative potential as measured by DTT was observed for summer ambient samples. In the same
468 study, correlations between ROS/RNS production and organic species were also observed for
469 summer ambient samples, and it was suggested that these correlations may reflect contributions
470 from photochemically produced SOA (Tuet et al., 2016).

471 Fig. 5 shows that laboratory-generated SOA oxidative potential is comparable to that
472 observed in ambient samples, with the exception of naphthalene SOA, which produced higher
473 DTT activities due to its aromatic ring retaining products (Tuet et al., 2017; Kautzman et al., 2010).
474 Laboratory-generated SOA also induced similar or higher levels of ROS/RNS compared to
475 ambient samples. There are many possible explanations for the observed higher response for some
476 SOA samples. For instance, individual, single precursor SOA systems were considered in this
477 study, whereas ambient aerosol contains SOA from multiple precursors as well as other species
478 that are not considered in this study (e.g. metals). Interactions between SOA from different
479 precursors is likely to occur and may result in different response levels. Complex interactions
480 between SOA and other species present in the ambient (e.g. metals or other organic species) are
481 also likely involved (Tuet et al., 2016). Previous studies have also suggested the possibility of
482 metal-organic complexes. For instance, Verma et al. (2012) showed that certain metals were
483 retained on a C-18 column, which is utilized to remove hydrophobic components, suggesting that
484 these metals were likely complexed and removed in the process. Further chamber studies involving
485 photochemically generated SOA and metals may elucidate these interactions. Furthermore, there
486 are likely species present in the ambient that do not contribute to ROS/RNS production. That is,
487 while certain species contribute to the mass of PM, there is little to no ROS/RNS production
488 associated with these species. Ambient samples where these species comprise a significant fraction
489 will have a low per mass ROS/RNS production level. Finally, only three SOA formation conditions

490 were investigated in this study. There are multiple other possible oxidation mechanisms that lead
491 to the formation of SOA in the ambient, which were not accounted for in this study. Nonetheless,
492 despite the low ROS/RNS levels observed post SOA exposure, there is an association between
493 ROS/RNS production and DTT activity (Fig. 5). These results suggest that our previous findings
494 based on ambient filter samples may be extended to SOA samples. That is, while the relationship
495 between ROS/RNS production and DTT activity is complex, DTT may serve as a useful screening
496 tool as samples with low DTT activities are likely to produce low levels of ROS/RNS (Tuet et al.,
497 2016).

498 **Implications.** Levels of ROS/RNS, TNF- α , and IL-6 were measured after exposing cells
499 to the water-soluble extract of SOA generated from the photooxidation of six SOA precursors
500 under various formation conditions. Although previous epidemiological and ambient studies have
501 found correlations between metals and various measures of health effects (Verma et al., 2010;
502 Pardo et al., 2015; Burnett et al., 2001; Huang et al., 2003; Akhtar et al., 2010; Charrier and
503 Anastasio, 2012), the measured levels of TNF- α , IL-6, and ROS/RNS obtained in this study
504 demonstrate that organic aerosols alone can induce a cellular response. This was previously
505 observed for the oxidative potential as measured by DTT activity as well, where the same
506 laboratory-generated organic aerosol samples catalyzed redox reactions and resulted in
507 measureable DTT decay in the absence of metal species (Tuet et al., 2017).

508 Results from this study also show that SOA precursor identity and formation condition
509 influenced response levels, with naphthalene SOA producing the highest cellular responses of the
510 SOA systems investigated. As discussed previously, the aromatic functionality present in many
511 naphthalene photooxidation products may be an important consideration for health effects. It may
512 therefore be worthwhile to investigate other anthropogenic aromatic ring-containing precursors as

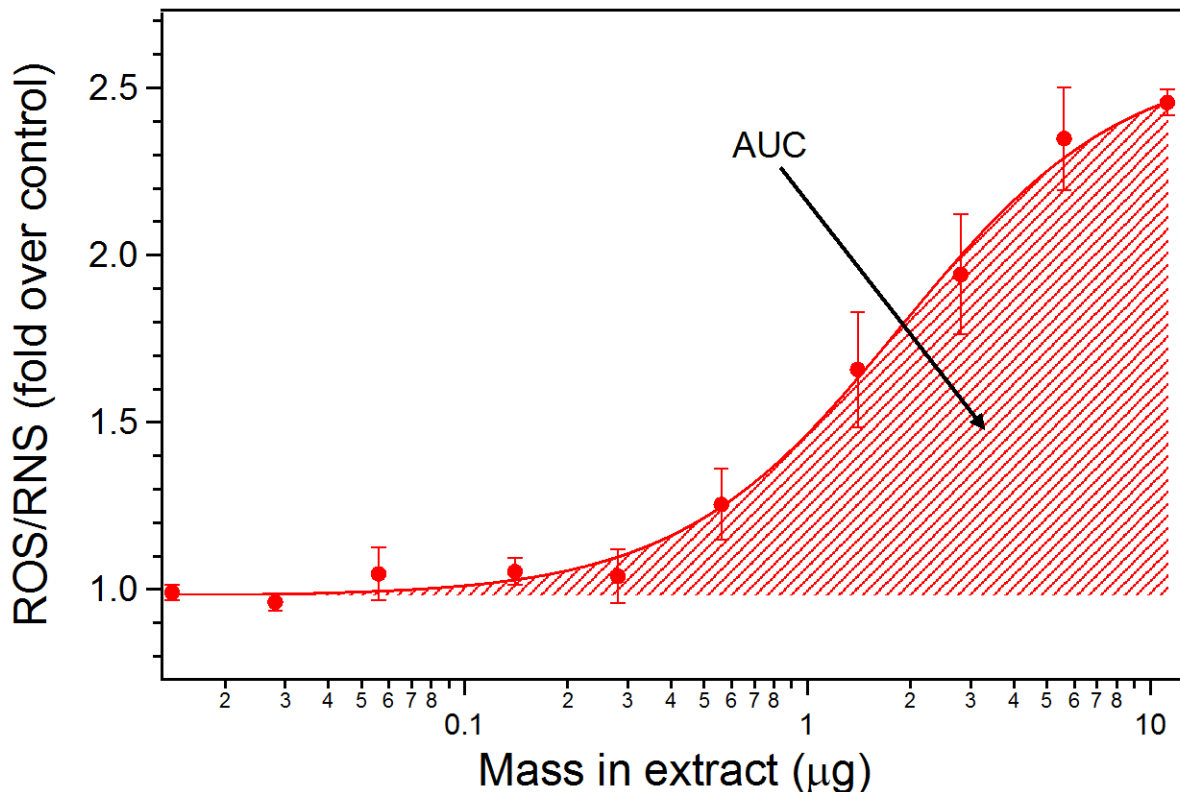
513 well and to closely study the cellular effects of naphthalene SOA products given its high response.
514 Several patterns were also noted for SOA systems whose products shared similar functionalities
515 and chemical structures. For instance, photooxidation productions from pentadecane and β -
516 caryophyllene share similarities with long chain fatty acids and may participate in membrane
517 insertions, whereas many known products of naphthalene photooxidation are mutagens capable of
518 inducing cellular pathways beyond those that affect cellular redox balance (Baird et al., 2005;
519 Helwig et al., 1992). Given these observations, it may be possible to roughly predict responses
520 based on known SOA products as SOA systems whose products share similar functionalities and
521 carbon chain length are likely to induce similar cellular pathways and produce similar levels of
522 various inflammatory endpoints. Exposure studies involving individual classes of SOA products
523 may elucidate further details as to whether these types of predictions would be plausible.
524 Moreover, such studies could be used to determine whether the hypothesized cellular pathways
525 are indeed involved and whether certain cellular functions are indeed affected by specific products
526 (e.g. membrane insertion by pentadecane photooxidation products and oxidative phosphorylation
527 decoupling by naphthalene photooxidation products).

528 Mixture effects may be another important consideration as ambient PM contains SOA
529 formed from multiple SOA precursors. As a result, precursor emissions and their corresponding
530 SOA formation potential must be considered to fully assess PM health effects. Furthermore, it may
531 be worthwhile to investigate various prediction models for multi-component mixtures to bridge
532 the gap between laboratory studies and real ambient exposures. For instance, concentration
533 addition may not apply as ambient aerosol is formed in the presence of multiple precursors and the
534 SOA produced may induce response levels completely different from those observed for single
535 precursor SOA systems that comprise the mixture. Interactions between organic components and

536 metal species have also been suggested in previous studies (Verma et al., 2012; Tuet et al., 2016)
537 and may influence responses significantly. While these interactions were not considered in the
538 current study, there may be evidence to support the plausibility of mixture effects as ambient PM
539 samples produced lower levels of ROS/RNS than that of any single SOA system investigated.
540 Laboratory chambers can serve as an ideal platform to investigate mixture effects, as experiments
541 can be conducted under well-controlled conditions where the aerosol chemical composition and
542 health endpoints can be determined.

543 Additionally, this study confirms that while there is not one simple correlation between
544 oxidative potential and cellular responses for different PM samples, the DTT assay may serve as
545 a useful screening tool as a low DTT activity will likely correspond to a low cellular response.
546 Furthermore, while ROS/RNS may serve as a general indicator of oxidative stress, there may be
547 instances where a low level of ROS/RNS does not necessary indicate a lack of cellular response.
548 In the current study, ROS/RNS levels were associated with levels of inflammatory cytokines for
549 the majority of SOA systems investigated. However, aerosol formed from the photooxidation of
550 pentadecane induced low levels of ROS/RNS production and relatively high levels of both
551 cytokines (i.e. higher than expected given the ROS/RNS level measured). These results suggest
552 that at least one additional measure (e.g. inflammatory cytokines) may be required to fully interpret
553 ROS/RNS measurements. Finally, several limitations must be considered before generalizing
554 results from this study to *in vivo* exposures. For instance, only one cell type was explored in this
555 study, whereas an organism consists of multiple tissues comprised of multiple cell types.
556 Interactions between different cell types and tissue systems were not considered in this study.
557 Furthermore, the doses investigated may not fully represent real world exposures due to
558 differences in exposure routes and potential recovery from doses due to clearance. Nevertheless,

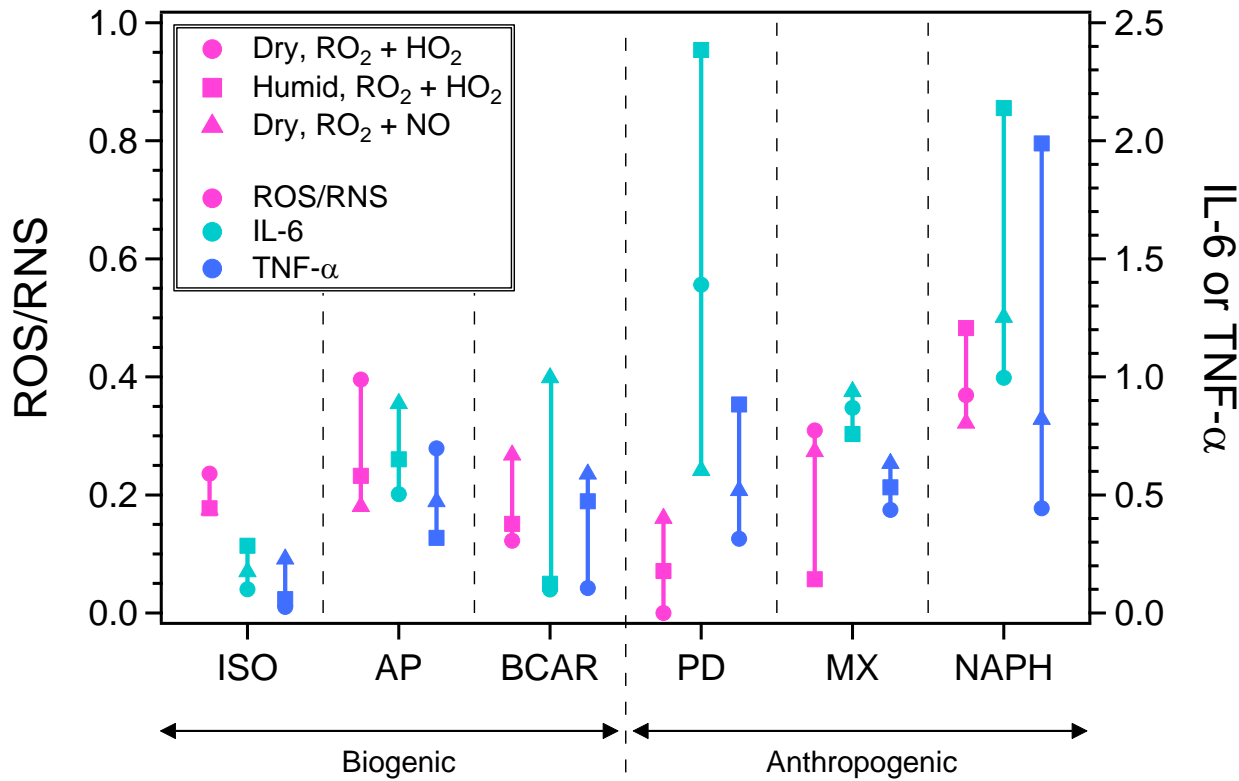
559 this study provides perspective on the relative toxicities of different SOA systems which future
560 studies can build upon.



561

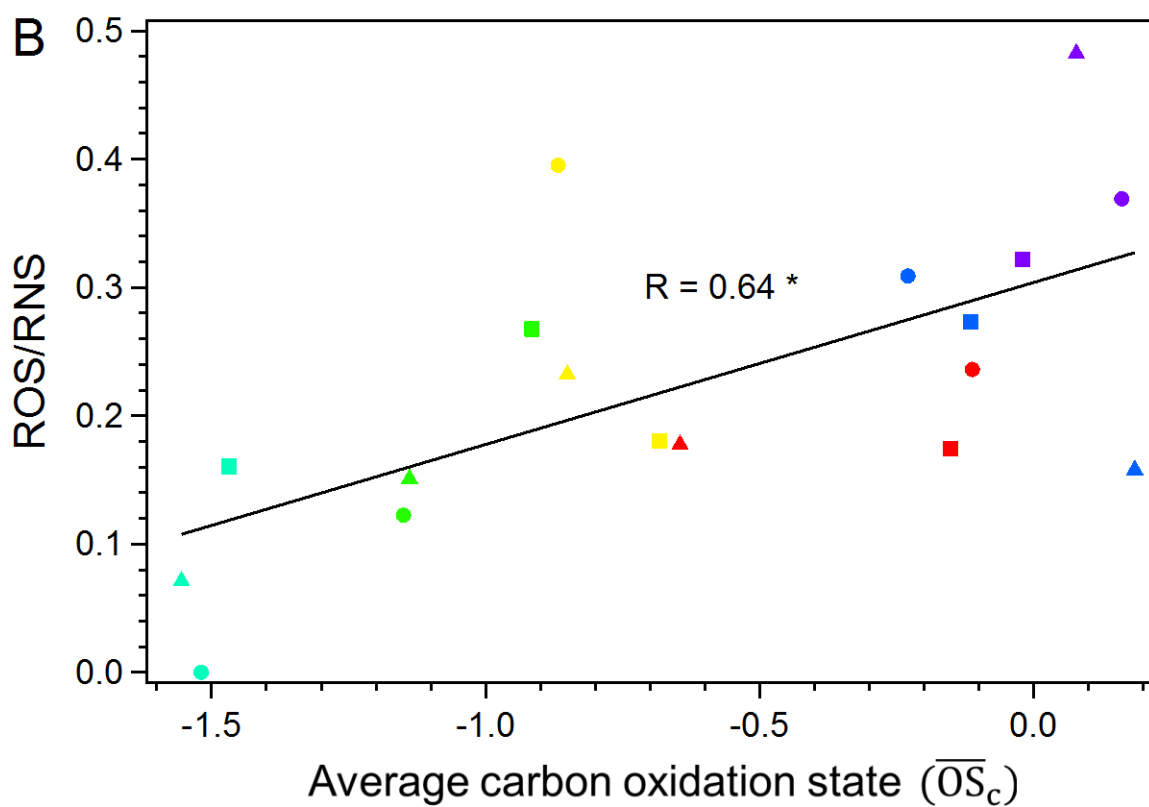
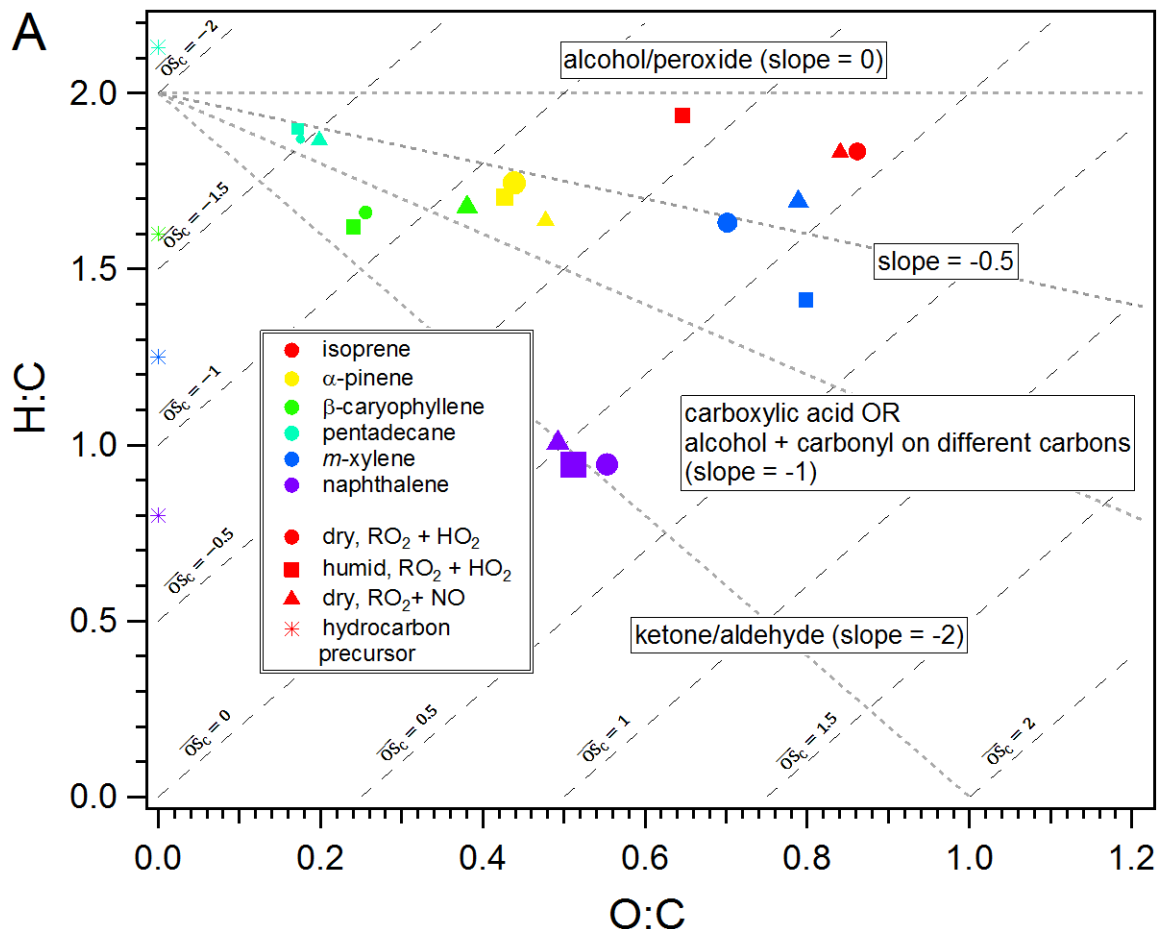
562 **Figure 1.** Representative dose-response curve of ROS/RNS produced as a result of filter
 563 exposure (naphthalene SOA formed under dry, RO₂ + NO dominant conditions). ROS/RNS is
 564 expressed as a fold increase over control cells, defined as probe-treated cells incubated with
 565 stimulant-free media. Dose is expressed as mass in extract (μg). Data shown are means ±
 566 standard error of triplicate exposure experiments. The Hill equation was used to fit the dose-
 567 response curve and the area under the dose-response curve (AUC) is shown.

568

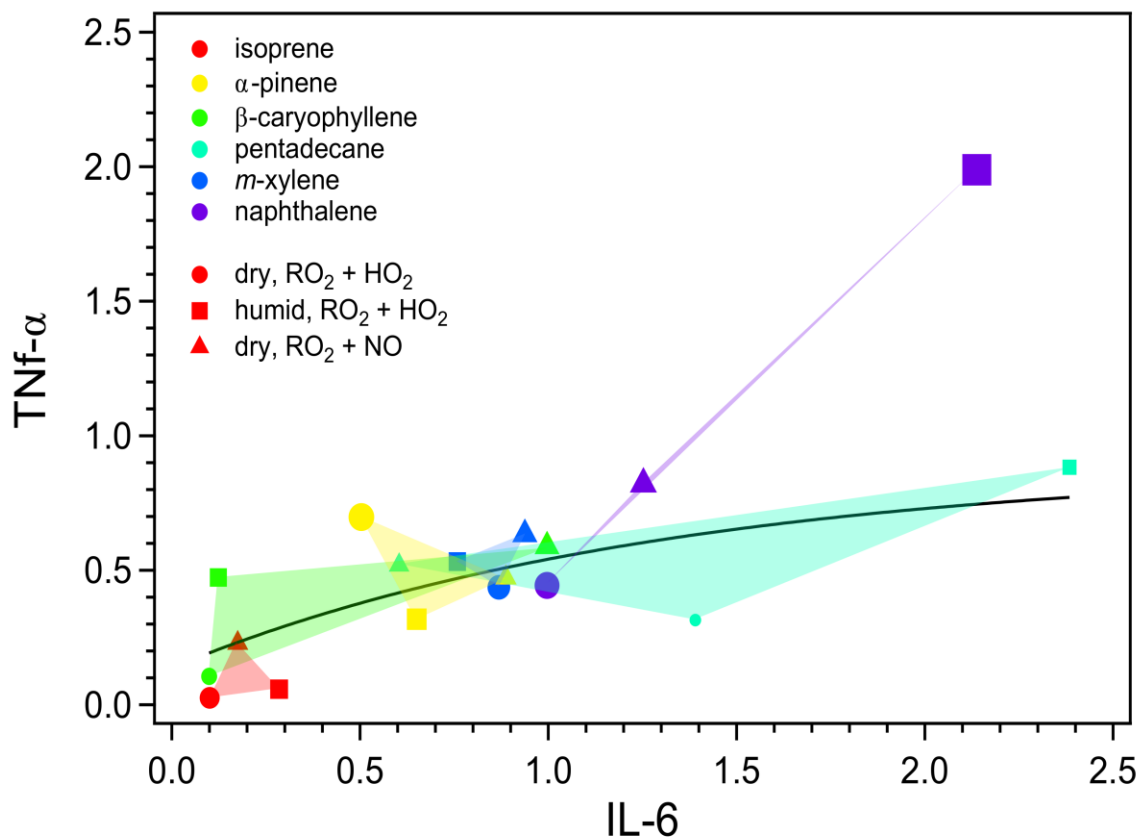


569

570 **Figure 2.** Area under the dose-response curve for various inflammatory responses induced as a
 571 result of SOA exposure: **ROS/RNS**, **IL-6**, and **TNF- α** . SOA were generated from various
 572 precursors (ISO: isoprene, AP: α -pinene, BCAR: β -caryophyllene, PD: pentadecane, MX: *m*-
 573 xylene, and NAPH: naphthalene) under various conditions (circles: dry, RO₂ + HO₂; squares:
 574 humid, RO₂ + HO₂; and triangles: dry, RO₂ + NO). Lines connecting the same inflammatory
 575 response for SOA generated from the same precursor under different formation conditions are also
 576 shown.

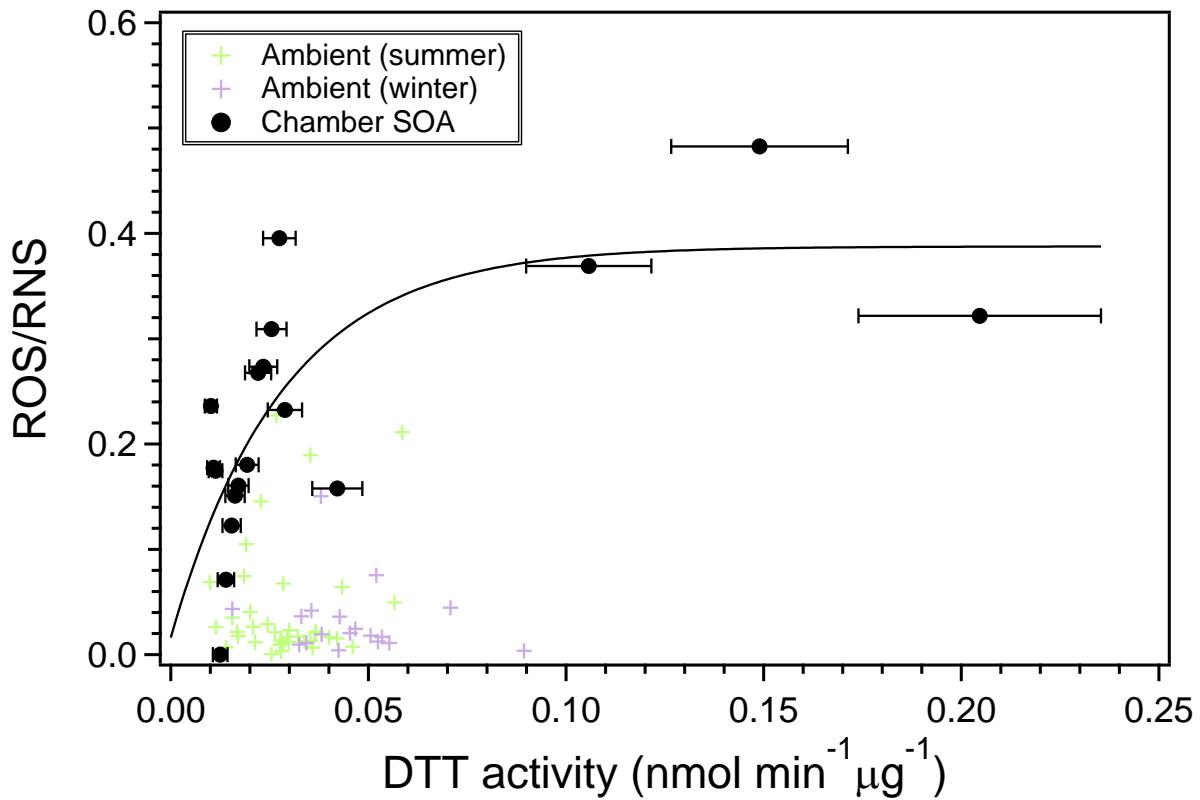


578 **Figure 3.** van Krevelen plot for various SOA systems sized by ROS/RNS levels (panel A) and
579 correlation between ROS/RNS levels and average carbon oxidation state (panel B). Data points
580 are colored by SOA system (red: isoprene, yellow: α -pinene, green: β -caryophyllene, light blue:
581 pentadecane, blue: *m*-xylene, and purple: naphthalene), shaped according to formation conditions
582 (circle: dry, $\text{RO}_2 + \text{HO}_2$; square: humid, $\text{RO}_2 + \text{HO}_2$; and triangle: dry, $\text{RO}_2 + \text{NO}$). SOA precursors
583 are shown as stars, colored by SOA system. * indicates significance, $p < 0.05$.



584

585 **Figure 4.** Area under the dose-response curve per mass of SOA for various inflammatory
 586 responses induced as a result of SOA exposure. Data points are sized according to ROS/RNS level.
 587 SOA were generated from various SOA precursors (red: isoprene, yellow: α -pinene, green: β -
 588 caryophyllene, light blue: pentadecane, blue: *m*-xylene, and purple: naphthalene) under various
 589 conditions (circles: dry, $\text{RO}_2 + \text{HO}_2$; squares: humid, $\text{RO}_2 + \text{HO}_2$; and triangles: dry, $\text{RO}_2 + \text{NO}$).
 590 A fitted curve excluding naphthalene data is shown as a guide. Shaded regions for each system,
 591 colored by SOA precursor, are also shown to show the extent of clustering and provide a
 592 visualization for the different patterns observed.



593

594 **Figure 5.** ROS/RNS production and intrinsic DTT activities for chamber SOA and ambient
 595 samples collected around the greater Atlanta area. All samples were analyzed using the method
 596 outlined in Cho et al. (2005) and Tuet et al. (2016). Ambient samples are colored by season as
 597 determined by solstice and equinox dates between June 2012 and October 2013 (Tuet et al.,
 598 2016). A fitted curve for laboratory-generated samples is shown as a guide.

599 **Table 1.** Experimental conditions.

| Experiment | SOA precursor | OH precursor | Relative humidity (%) | [HC] ₀ (ppb) |
|------------|------------------|-------------------------------|-----------------------|-------------------------|
| 1 | isoprene | H ₂ O ₂ | <5% | 97 |
| 2 | α-pinene | H ₂ O ₂ | <5% | 191 |
| 3 | β-caryophyllene | H ₂ O ₂ | <5% | 36 |
| 4 | pentadecane | H ₂ O ₂ | <5% | 106 |
| 5 | <i>m</i> -xylene | H ₂ O ₂ | <5% | 450 |
| 6 | naphthalene | H ₂ O ₂ | <5% | 178 |
| 7 | isoprene | H ₂ O ₂ | <5% ^a | 97 |
| 8 | α-pinene | H ₂ O ₂ | 40% | 334 |
| 9 | β-caryophyllene | H ₂ O ₂ | 42% | 63 |
| 10 | pentadecane | H ₂ O ₂ | 45% | 106 |
| 11 | <i>m</i> -xylene | H ₂ O ₂ | 45% | 450 |
| 12 | naphthalene | H ₂ O ₂ | 44% | 431 |
| 13 | isoprene | HONO | <5% | 970 |
| 14 | α-pinene | HONO | <5% | 174 |
| 15 | β-caryophyllene | HONO | <5% | 21 |
| 16 | pentadecane | HONO | <5% | 74 |
| 17 | <i>m</i> -xylene | HONO | <5% | 431 |
| 18 | naphthalene | HONO | <5% | 145 |

600 ^a Acidic seed (8 mM MgSO₄ and 16 mM H₂SO₄) was used instead of 8 mM (NH₄)₂SO₄

601 ACKNOWLEDGMENT

602 This work was supported by the Health Effects Institute under research agreement No. 4943-
603 RFA13-2/14-4. Wing Y. Tuet acknowledges support by the National Science Foundation
604 Graduate Research Fellowship under Grant No. DGE-1650044.

605 ABBREVIATIONS

606 PM: particulate matter; SOA: secondary organic aerosol; ROS/RNS: reactive oxygen/nitrogen
607 species; TNF- α : tumor necrosis factor- α ; IL-6: interleukin-6

608 REFERENCES

609 Akhtar, U. S., McWhinney, R. D., Rastogi, N., Abbatt, J. P., Evans, G. J., and Scott, J. A.:
610 Cytotoxic and proinflammatory effects of ambient and source-related particulate matter (PM) in
611 relation to the production of reactive oxygen species (ROS) and cytokine adsorption by particles,
612 *Inhal. Toxicol.*, 22, 37-47, 2010.

613 Anderson, J. O., Thundiyil, J. G., and Stolbach, A.: Clearing the Air: A Review of the Effects of
614 Particulate Matter Air Pollution on Human Health, *Journal of Medical Toxicology*, 8, 166-175,
615 10.1007/s13181-011-0203-1, 2011.

616 Arashiro, M., Lin, Y. H., Sexton, K. G., Zhang, Z., Jaspers, I., Fry, R. C., Vizuete, W. G., Gold,
617 A., and Surratt, J. D.: In Vitro Exposure to Isoprene-Derived Secondary Organic Aerosol by
618 Direct Deposition and its Effects on COX-2 and IL-8 Gene Expression, *Atmos. Chem. Phys.*
619 *Discuss.*, 2016, 1-29, 10.5194/acp-2016-371, 2016.

620 Baird, W. M., Hooven, L. A., and Mahadevan, B.: Carcinogenic polycyclic aromatic
621 hydrocarbon-DNA adducts and mechanism of action, *Environmental and Molecular*
622 *Mutagenesis*, 45, 106-114, 10.1002/em.20095, 2005.

623 Baltensperger, U., Dommen, J., Alfarra, R., Duplissy, J., Gaeggeler, K., Metzger, A., Facchini,
624 M. C., Decesari, S., Finessi, E., Reinnig, C., Schott, M., Warnke, J., Hoffmann, T., Klatzer, B.,
625 Puxbaum, H., Geiser, M., Savi, M., Lang, D., Kalberer, M., and Geiser, T.: Combined
626 determination of the chemical composition and of health effects of secondary organic aerosols:
627 The POLYSOA project, *J. Aerosol Med. Pulm. Drug Deliv.*, 21, 145-154,
628 10.1089/jamp.2007.0655, 2008.

629 Baritaki, S., Apostolakis, S., Kanellou, P., Dimanche-Boitrel, M. T., Spandidos, D. A., and
630 Bonavida, B.: Reversal of Tumor Resistance to Apoptotic Stimuli by Alteration of Membrane
631 Fluidity: Therapeutic Implications, in: *Advances in Cancer Research*, Academic Press, 149-190,
632 2007.

633 Bates, J. T., Weber, R. J., Abrams, J., Verma, V., Fang, T., Klein, M., Strickland, M. J., Sarnat,
634 S. E., Chang, H. H., Mulholland, J. A., Tolbert, P. E., and Russell, A. G.: Reactive Oxygen
635 Species Generation Linked to Sources of Atmospheric Particulate Matter and Cardiorespiratory
636 Effects, *Environmental Science & Technology*, 49, 13605-13612, 10.1021/acs.est.5b02967,
637 2015.

638 Boyd, C. M., Sanchez, J., Xu, L., Eugene, A. J., Nah, T., Tuet, W. Y., Guzman, M. I., and Ng, N.
639 L.: Secondary organic aerosol formation from the β -pinene+NO₃ system: effect of
640 humidity and peroxy radical fate, *Atmos. Chem. Phys.*, 15, 7497-7522, 10.5194/acp-15-7497-
641 2015, 2015.

642 Brunekreef, B., and Holgate, S. T.: Air pollution and health, *Lancet*, 360, 1233-1242, 2002.

643 Bruns, E. A., El Haddad, I., Slowik, J. G., Kilic, D., Klein, F., Baltensperger, U., and Prévôt, A.
644 S. H.: Identification of significant precursor gases of secondary organic aerosols from residential
645 wood combustion, *Scientific Reports*, 6, 27881, 10.1038/srep27881

646 <http://www.nature.com/articles/srep27881#supplementary-information>, 2016.

647 Burnett, R., Brook, J., Dann, T., Delocla, C., Philips, O., Cakmak, S., Vincent, R., Goldberg, M.,
648 and Krewski, D.: Association between particulate-and gas-phase components of urban air
649 pollution and daily mortality in eight Canadian cities, 2001.

650 Canagaratna, M. R., Jimenez, J. L., Kroll, J. H., Chen, Q., Kessler, S. H., Massoli, P.,
651 Hildebrandt Ruiz, L., Fortner, E., Williams, L. R., Wilson, K. R., Surratt, J. D., Donahue, N. M.,
652 Jayne, J. T., and Worsnop, D. R.: Elemental ratio measurements of organic compounds using
653 aerosol mass spectrometry: characterization, improved calibration, and implications, *Atmos.*
654 *Chem. Phys.*, 15, 253-272, 10.5194/acp-15-253-2015, 2015.

655 Castro, L., and Freeman, B. A.: Reactive oxygen species in human health and disease, *Nutrition*,
656 17, 161-165, 2001.

657 Cerezo, J., Zúñiga, J., Bastida, A., Requena, A., and Cerón-Carrasco, J. P.: Atomistic Molecular
658 Dynamics Simulations of the Interactions of Oleic and 2-Hydroxyoleic Acids with
659 Phosphatidylcholine Bilayers, *The Journal of Physical Chemistry B*, 115, 11727-11738,
660 10.1021/jp203498x, 2011.

661 Chan, A. W. H., Kautzman, K. E., Chhabra, P. S., Surratt, J. D., Chan, M. N., Crounse, J. D.,
662 Kurten, A., Wennberg, P. O., Flagan, R. C., and Seinfeld, J. H.: Secondary organic aerosol
663 formation from photooxidation of naphthalene and alkynaphthalenes: implications for oxidation
664 of intermediate volatility organic compounds (IVOCs), *Atmos. Chem. Phys.*, 9, 3049-3060,
665 2009.

666 Chan, A. W. H., Chan, M. N., Surratt, J. D., Chhabra, P. S., Loza, C. L., Crounse, J. D., Yee, L.
667 D., Flagan, R. C., Wennberg, P. O., and Seinfeld, J. H.: Role of aldehyde chemistry and
668 NO_x concentrations in secondary organic aerosol formation, *Atmos. Chem. Phys.*, 10, 7169-7188, 10.5194/acp-10-7169-2010, 2010.

670 Chan, M. N., Surratt, J. D., Chan, A. W. H., Schilling, K., Offenberg, J. H., Lewandowski, M.,
671 Edney, E. O., Kleindienst, T. E., Jaoui, M., Edgerton, E. S., Tanner, R. L., Shaw, S. L., Zheng,
672 M., Knipping, E. M., and Seinfeld, J. H.: Influence of aerosol acidity on the chemical
673 composition of secondary organic aerosol from β -caryophyllene, *Atmos. Chem. Phys.*, 11,
674 1735-1751, 10.5194/acp-11-1735-2011, 2011.

675 Charrier, J. G., and Anastasio, C.: On dithiothreitol (DTT) as a measure of oxidative potential for
676 ambient particles: evidence for the importance of soluble transition metals, *Atmos. Chem. Phys.*,
677 12, 9321-9333, 10.5194/acp-12-9321-2012, 2012.

678 Chen, C. Y., Peng, W. H., Tsai, K. D., and Hsu, S. L.: Luteolin suppresses inflammation-
679 associated gene expression by blocking NF-kappa B and AP-1 activation pathway in mouse
680 alveolar macrophages, *Life Sci.*, 81, 1602-1614, 10.1016/j.lfs.2007.09.028, 2007.

681 Chhabra, P. S., Flagan, R. C., and Seinfeld, J. H.: Elemental analysis of chamber organic aerosol
682 using an aerodyne high-resolution aerosol mass spectrometer, *Atmos. Chem. Phys.*, 10, 4111-
683 4131, 10.5194/acp-10-4111-2010, 2010.

684 Chhabra, P. S., Ng, N. L., Canagaratna, M. R., Corrigan, A. L., Russell, L. M., Worsnop, D. R.,
685 Flagan, R. C., and Seinfeld, J. H.: Elemental composition and oxidation of chamber organic
686 aerosol, *Atmos. Chem. Phys.*, 11, 8827-8845, 10.5194/acp-11-8827-2011, 2011.

687 Cho, A. K., Sioutas, C., Miguel, A. H., Kumagai, Y., Schmitz, D. A., Singh, M., Eiguren-
688 Fernandez, A., and Froines, J. R.: Redox activity of airborne particulate matter at different sites
689 in the Los Angeles Basin, *Environmental Research*, 99, 40-47, 10.1016/j.envres.2005.01.003,
690 2005.

691 Cocker III, D. R., Mader, B. T., Kalberer, M., Flagan, R. C., and Seinfeld, J. H.: The effect of
692 water on gas-particle partitioning of secondary organic aerosol: II. m-xylene and 1,3,5-
693 trimethylbenzene photooxidation systems, *Atmos. Environ.*, 35, 6073-6085,
694 [http://dx.doi.org/10.1016/S1352-2310\(01\)00405-8](http://dx.doi.org/10.1016/S1352-2310(01)00405-8), 2001.

695 DeCarlo, P. F., Kimmel, J. R., Trimborn, A., Northway, M. J., Jayne, J. T., Aiken, A. C., Gonin,
696 M., Fuhrer, K., Horvath, T., Docherty, K. S., Worsnop, D. R., and Jimenez, J. L.: Field-
697 Deployable, High-Resolution, Time-of-Flight Aerosol Mass Spectrometer, *Analytical Chemistry*,
698 78, 8281-8289, 10.1021/ac061249n, 2006.

699 Dockery, D. W., Pope, C. A., Xu, X., Spengler, J. D., Ware, J. H., Fay, M. E., Ferris, B. G., and
700 Speizer, F. E.: An Association between Air Pollution and Mortality in Six U.S. Cities, *New
701 England Journal of Medicine*, 329, 1753-1759, doi:10.1056/NEJM199312093292401, 1993.

702 Eddingsaas, N. C., Loza, C. L., Yee, L. D., Chan, M., Schilling, K. A., Chhabra, P. S., Seinfeld,
703 J. H., and Wennberg, P. O.: α -pinene photooxidation under controlled chemical conditions
704 – Part 2: SOA yield and composition in low- and high-NO_x environments, *Atmos. Chem.
705 Phys.*, 12, 7413-7427, 10.5194/acp-12-7413-2012, 2012.

706 Edney, E. O., Driscoll, D. J., Speer, R. E., Weathers, W. S., Kleindienst, T. E., Li, W., and
707 Smith, D. F.: Impact of aerosol liquid water on secondary organic aerosol yields of irradiated
708 toluene/propylene/NO_x/(NH₄)₂SO₄/air mixtures, *Atmos. Environ.*, 34, 3907-3919,
709 [http://dx.doi.org/10.1016/S1352-2310\(00\)00174-6](http://dx.doi.org/10.1016/S1352-2310(00)00174-6), 2000.

710 Fang, T., Guo, H., Verma, V., Peltier, R. E., and Weber, R. J.: PM2.5 water-soluble elements in
711 the southeastern United States: automated analytical method development, spatiotemporal
712 distributions, source apportionment, and implications for health studies, *Atmos. Chem. Phys.*, 15,
713 11667-11682, 10.5194/acp-15-11667-2015, 2015a.

714 Fang, T., Verma, V., Guo, H., King, L. E., Edgerton, E. S., and Weber, R. J.: A semi-automated
715 system for quantifying the oxidative potential of ambient particles in aqueous extracts using the

716 dithiothreitol (DTT) assay: results from the Southeastern Center for Air Pollution and
717 Epidemiology (SCAPE), *Atmos. Meas. Tech.*, 8, 471-482, 10.5194/amt-8-471-2015, 2015b.

718 Gallimore, P. J., Mahon, B. M., Wragg, F. P. H., Fuller, S. J., Giorio, C., Kourtchev, I., and
719 Kalberer, M.: Multiphase composition changes and reactive oxygen species formation during
720 limonene oxidation in the new Cambridge Atmospheric Simulation Chamber (CASC), *Atmos.*
721 *Chem. Phys. Discuss.*, 2017, 1-30, 10.5194/acp-2017-186, 2017.

722 Goldstein, A. H., and Galbally, I. E.: Known and Unexplored Organic Constituents in the Earth's
723 Atmosphere, *Environmental Science & Technology*, 41, 1514-1521, 10.1021/es072476p, 2007.

724 Guenther, A., Karl, T., Harley, P., Wiedinmyer, C., Palmer, P. J., and Geron, C.: Estimates of
725 global terrestrial isoprene emissions using MEGAN (Model of Emissions of Gases and Aerosols
726 from Nature), *Atmos. Chem. Phys.*, 6, 3181-3210, 10.5194/acp-6-3181-2006, 2006.

727 Guenther, A. B., Zimmerman, P. R., Harley, P. C., Monson, R. K., and Fall, R.: Isoprene and
728 monoterpene emission rate variability: Model evaluations and sensitivity analyses, *Journal of*
729 *Geophysical Research: Atmospheres*, 98, 12609-12617, 10.1029/93JD00527, 1993.

730 Gurgueira, S. A., Lawrence, J., Coull, B., Murthy, G. G. K., and Gonzalez-Flecha, B.: Rapid
731 increases in the steady-state concentration of reactive oxygen species in the lungs and heart after
732 particulate air pollution inhalation, *Environmental Health Perspectives*, 110, 749-755, 2002.

733 Haddad, J. J.: L-buthionine-(S,R)-sulfoximine, an irreversible inhibitor of gamma-
734 glutamylcysteine synthetase, augments LPS-mediated pro-inflammatory cytokine biosynthesis:
735 evidence for the implication of an I kappa B-alpha/NF-kappa B insensitive pathway, *Eur.*
736 *Cytokine Netw.*, 12, 614-624, 2001.

737 Hamad, S. H., Shafer, M. M., Kadhim, A. K. H., Al-Omran, S. M., and Schauer, J. J.: Seasonal
738 trends in the composition and ROS activity of fine particulate matter in Baghdad, Iraq, *Atmos.*
739 *Environ.*, 100, 102-110, <http://dx.doi.org/10.1016/j.atmosenv.2014.10.043>, 2015.

740 Heald, C. L., Kroll, J. H., Jimenez, J. L., Docherty, K. S., DeCarlo, P. F., Aiken, A. C., Chen, Q.,
741 Martin, S. T., Farmer, D. K., and Artaxo, P.: A simplified description of the evolution of organic
742 aerosol composition in the atmosphere, *Geophysical Research Letters*, 37, n/a-n/a,
743 10.1029/2010GL042737, 2010.

744 Healy, R. M., Temime, B., Kuprovskaite, K., and Wenger, J. C.: Effect of Relative Humidity on
745 Gas/Particle Partitioning and Aerosol Mass Yield in the Photooxidation of p-Xylene,
746 *Environmental Science & Technology*, 43, 1884-1889, 10.1021/es802404z, 2009.

747 Helming, D., Arey, J., Harger, W. P., Atkinson, R., and Lopez-Cancio, J.: Formation of mutagenic
748 nitrodibenzopyranones and their occurrence in ambient air, *Environmental Science &*
749 *Technology*, 26, 622-624, 10.1021/es00027a028, 1992.

750 Henkler, F., Brinkmann, J., and Luch, A.: The Role of Oxidative Stress in Carcinogenesis
751 Induced by Metals and Xenobiotics, *Cancers*, 2, 376, 2010.

752 Hensley, K., Robinson, K. A., Gabbita, S. P., Salsman, S., and Floyd, R. A.: Reactive oxygen
753 species, cell signaling, and cell injury, *Free Radical Biology and Medicine*, 28, 1456-1462,
754 [http://dx.doi.org/10.1016/S0891-5849\(00\)00252-5](http://dx.doi.org/10.1016/S0891-5849(00)00252-5), 2000.

755 Hoek, G., Krishnan, R. M., Beelen, R., Peters, A., Ostro, B., Brunekreef, B., and Kaufman, J. D.:
756 Long-term air pollution exposure and cardio-respiratory mortality: a review, *Environ Health*, 12,
757 43, 2013.

758 Hoffmann, T., Odum, J., Bowman, F., Collins, D., Klockow, D., Flagan, R., and Seinfeld, J.:
759 Formation of Organic Aerosols from the Oxidation of Biogenic Hydrocarbons, *Journal of*
760 *Atmospheric Chemistry*, 26, 189-222, 10.1023/A:1005734301837, 1997.

761 Huang, Y.-C. T., Ghio, A. J., Stonehuerer, J., McGee, J., Carter, J. D., Grambow, S. C., and
762 Devlin, R. B.: The role of soluble components in ambient fine particles-induced changes in
763 human lungs and blood, *Inhal. Toxicol.*, 15, 327-342, 2003.

764 Jenkin, M. E., Saunders, S. M., Wagner, V., and Pilling, M. J.: Protocol for the development of
765 the Master Chemical Mechanism, MCM v3 (Part B): tropospheric degradation of aromatic
766 volatile organic compounds, *Atmos. Chem. Phys.*, 3, 181-193, 10.5194/acp-3-181-2003, 2003.

767 Jia, C., and Batterman, S.: A Critical Review of Naphthalene Sources and Exposures Relevant to
768 Indoor and Outdoor Air, *International Journal of Environmental Research and Public Health*, 7,
769 2903-2939, 10.3390/ijerph7072903, 2010.

770 Jimenez, J. L., Canagaratna, M. R., Donahue, N. M., Prevot, A. S. H., Zhang, Q., Kroll, J. H.,
771 DeCarlo, P. F., Allan, J. D., Coe, H., Ng, N. L., Aiken, A. C., Docherty, K. S., Ulbrich, I. M.,
772 Grieshop, A. P., Robinson, A. L., Duplissy, J., Smith, J. D., Wilson, K. R., Lanz, V. A., Hueglin,
773 C., Sun, Y. L., Tian, J., Laaksonen, A., Raatikainen, T., Rautiainen, J., Vaattovaara, P., Ehn, M.,
774 Kulmala, M., Tomlinson, J. M., Collins, D. R., Cubison, M. J., Dunlea, J., Huffman, J. A.,
775 Onasch, T. B., Alfarra, M. R., Williams, P. I., Bower, K., Kondo, Y., Schneider, J., Drewnick, F.,
776 Borrmann, S., Weimer, S., Demerjian, K., Salcedo, D., Cottrell, L., Griffin, R., Takami, A.,
777 Miyoshi, T., Hatakeyama, S., Shimono, A., Sun, J. Y., Zhang, Y. M., Dzepina, K., Kimmel, J.,
778 R., Sueper, D., Jayne, J. T., Herndon, S. C., Trimborn, A. M., Williams, L. R., Wood, E. C.,
779 Middlebrook, A. M., Kolb, C. E., Baltensperger, U., and Worsnop, D. R.: Evolution of Organic
780 Aerosols in the Atmosphere, *Science*, 326, 1525-1529, 10.1126/science.1180353, 2009.

781 Kamimura, D., Ishihara, K., and Hirano, T.: IL-6 signal transduction and its physiological roles:
782 the signal orchestration model, in: *Reviews of Physiology, Biochemistry and Pharmacology*,
783 Springer Berlin Heidelberg, Berlin, Heidelberg, 1-38, 2004.

784 Kautzman, K. E., Surratt, J. D., Chan, M. N., Chan, A. W. H., Hersey, S. P., Chhabra, P. S.,
785 Dalleska, N. F., Wennberg, P. O., Flagan, R. C., and Seinfeld, J. H.: Chemical Composition of
786 Gas- and Aerosol-Phase Products from the Photooxidation of Naphthalene, *The Journal of*
787 *Physical Chemistry A*, 114, 913-934, 10.1021/jp908530s, 2010.

788 Khmelinskaia, A., Ibarguren, M., de Almeida, R. F. M., López, D. J., Paixão, V. A., Ahyayauch,
789 H., Goñi, F. M., and Escribá, P. V.: Changes in Membrane Organization upon Spontaneous
790 Insertion of 2-Hydroxylated Unsaturated Fatty Acids in the Lipid Bilayer, *Langmuir*, 30, 2117-
791 2128, 10.1021/la403977f, 2014.

792 Kishimoto, T.: *Interleukin-6, The cytokine handbook*, 4, 281-304, 2003.

793 Kleinman, M. T., Hamade, A., Meacher, D., Oldham, M., Sioutas, C., Chakrabarti, B., Stram, D.,
794 Froines, J. R., and Cho, A. K.: Inhalation of concentrated ambient particulate matter near a
795 heavily trafficked road stimulates antigen-induced airway responses in mice, *Journal of the Air*
796 & Waste Management Association

797 Kramer, A. J., Rattanavaraha, W., Zhang, Z., Gold, A., Surratt, J. D., and Lin, Y.-H.: Assessing
798 the oxidative potential of isoprene-derived epoxides and secondary organic aerosol, *Atmos.*
799 *Environ.*, <http://dx.doi.org/10.1016/j.atmosenv.2015.10.018>, 2016.

800 Kroll, J. H., Ng, N. L., Murphy, S. M., Flagan, R. C., and Seinfeld, J. H.: Secondary organic
801 aerosol formation from isoprene photooxidation under high-NO_x conditions, *Geophysical*
802 *Research Letters*, 32, n/a-n/a, 10.1029/2005GL023637, 2005.

803 Kroll, J. H., Donahue, N. M., Jimenez, J. L., Kessler, S. H., Canagaratna, M. R., Wilson, K. R.,
804 Altieri, K. E., Mazzoleni, L. R., Wozniak, A. S., Bluhm, H., Mysak, E. R., Smith, J. D., Kolb, C.
805 E., and Worsnop, D. R.: Carbon oxidation state as a metric for describing the chemistry of
806 atmospheric organic aerosol, *Nat Chem*, 3, 133-139,
807 <http://www.nature.com/nchem/journal/v3/n2/abs/nchem.948.html#supplementary-information>,
808 2011.

809 Kumagai, Y., Koide, S., Taguchi, K., Endo, A., Nakai, Y., Yoshikawa, T., and Shimojo, N.:
810 Oxidation of proximal protein sulphydryls by phenanthraquinone, a component of diesel exhaust
811 particles, *Chemical Research in Toxicology*, 15, 483-489, 10.1021/tx0100993, 2002.

812 Lambe, A. T., Onasch, T. B., Massoli, P., Croasdale, D. R., Wright, J. P., Ahern, A. T.,
813 Williams, L. R., Worsnop, D. R., Brune, W. H., and Davidovits, P.: Laboratory studies of the
814 chemical composition and cloud condensation nuclei (CCN) activity of secondary organic
815 aerosol (SOA) and oxidized primary organic aerosol (OPOA), *Atmos. Chem. Phys.*, 11, 8913-
816 8928, 10.5194/acp-11-8913-2011, 2011.

817 Landreman, A. P., Shafer, M. M., Hemming, J. C., Hannigan, M. P., and Schauer, J. J.: A
818 macrophage-based method for the assessment of the reactive oxygen species (ROS) activity of
819 atmospheric particulate matter (PM) and application to routine (daily-24 h) aerosol monitoring
820 studies, *Aerosol Sci. Technol.*, 42, 946-957, 10.1080/02786820802363819, 2008.

821 Li, N., Hao, M. Q., Phalen, R. F., Hinds, W. C., and Nel, A. E.: Particulate air pollutants and
822 asthma - A paradigm for the role of oxidative stress in PM-induced adverse health effects,
823 *Clinical Immunology*, 109, 250-265, 10.1016/j.clim.2003.08.006, 2003a.

824 Li, N., Sioutas, C., Cho, A., Schmitz, D., Misra, C., Sempf, J., Wang, M. Y., Oberley, T.,
825 Froines, J., and Nel, A.: Ultrafine particulate pollutants induce oxidative stress and mitochondrial
826 damage, *Environmental Health Perspectives*, 111, 455-460, 10.1289/ehp.6000, 2003b.

827 Li, N., Xia, T., and Nel, A. E.: The role of oxidative stress in ambient particulate matter-induced
828 lung diseases and its implications in the toxicity of engineered nanoparticles, *Free Radical
829 Biology and Medicine*, 44, 1689-1699, 10.1016/j.freeradbiomed.2008.01.028, 2008.

830 Lim, S. S., Vos, T., Flaxman, A. D., Danaei, G., Shibuya, K., Adair-Rohani, H., AlMazroa, M.
831 A., Amann, M., Anderson, H. R., Andrews, K. G., Aryee, M., Atkinson, C., Bacchus, L. J.,
832 Bahalim, A. N., Balakrishnan, K., Balmes, J., Barker-Collo, S., Baxter, A., Bell, M. L., Blore, J.
833 D., Blyth, F., Bonner, C., Borges, G., Bourne, R., Boussinesq, M., Brauer, M., Brooks, P., Bruce,
834 N. G., Brunekreef, B., Bryan-Hancock, C., Bucello, C., Buchbinder, R., Bull, F., Burnett, R. T.,
835 Byers, T. E., Calabria, B., Carapetis, J., Carnahan, E., Chafe, Z., Charlson, F., Chen, H., Chen, J.
836 S., Cheng, A. T.-A., Child, J. C., Cohen, A., Colson, K. E., Cowie, B. C., Darby, S., Darling, S.,
837 Davis, A., Degenhardt, L., Dentener, F., Des Jarlais, D. C., Devries, K., Dherani, M., Ding, E. L.,
838 Dorsey, E. R., Driscoll, T., Edmond, K., Ali, S. E., Engell, R. E., Erwin, P. J., Fahimi, S., Falder,
839 G., Farzadfar, F., Ferrari, A., Finucane, M. M., Flaxman, S., Fowkes, F. G. R., Freedman, G.,

840 Freeman, M. K., Gakidou, E., Ghosh, S., Giovannucci, E., Gmel, G., Graham, K., Grainger, R.,
841 Grant, B., Gunnell, D., Gutierrez, H. R., Hall, W., Hoek, H. W., Hogan, A., Hosgood, H. D., III,
842 Hoy, D., Hu, H., Hubbell, B. J., Hutchings, S. J., Ibeanusi, S. E., Jacklyn, G. L., Jasrasaria, R.,
843 Jonas, J. B., Kan, H., Kanis, J. A., Kassebaum, N., Kawakami, N., Khang, Y.-H., Khatibzadeh, S.,
844 Khoo, J.-P., Kok, C., Laden, F., Laloo, R., Lan, Q., Lathlean, T., Leasher, J. L., Leigh, J., Li, Y.,
845 Lin, J. K., Lipshultz, S. E., London, S., Lozano, R., Lu, Y., Mak, J., Malekzadeh, R.,
846 Mallinger, L., Marcenés, W., March, L., Marks, R., Martin, R., McGale, P., McGrath, J., Mehta, S.,
847 Memish, Z. A., Mensah, G. A., Merriman, T. R., Micha, R., Michaud, C., Mishra, V.,
848 Hanafiah, K. M., Mokdad, A. A., Morawska, L., Mozaffarian, D., Murphy, T., Naghavi, M.,
849 Neal, B., Nelson, P. K., Nolla, J. M., Norman, R., Olives, C., Omer, S. B., Orchard, J., Osborne, R.,
850 Ostro, B., Page, A., Pandey, K. D., Parry, C. D. H., Passmore, E., Patra, J., Pearce, N.,
851 Pelizzari, P. M., Petzold, M., Phillips, M. R., Pope, D., Pope, C. A., III, Powles, J., Rao, M.,
852 Razavi, H., Rehfuss, E. A., Rehm, J. T., Ritz, B., Rivara, F. P., Roberts, T., Robinson, C.,
853 Rodriguez-Portales, J. A., Romieu, I., Room, R., Rosenfeld, L. C., Roy, A., Rushton, L.,
854 Salomon, J. A., Sampson, U., Sanchez-Riera, L., Sanman, E., Sapkota, A., Seedat, S., Shi, P.,
855 Shield, K., Shivakoti, R., Singh, G. M., Sleet, D. A., Smith, E., Smith, K. R., Stapelberg, N. J. C.,
856 Steenland, K., Stöckl, H., Stovner, L. J., Straif, K., Straney, L., Thurston, G. D., Tran, J. H.,
857 Van Dingenen, R., van Donkelaar, A., Veerman, J. L., Vijayakumar, L., Weintraub, R.,
858 Weissman, M. M., White, R. A., Whiteford, H., Wiersma, S. T., Wilkinson, J. D., Williams, H. C.,
859 Williams, W., Wilson, N., Woolf, A. D., Yip, P., Zielinski, J. M., Lopez, A. D., Murray, C. J. L., and Ezzati, M.: A comparative risk assessment of burden of disease and injury attributable to
860 67 risk factors and risk factor clusters in 21 regions, 1990–2010: a systematic analysis for the
861 Global Burden of Disease Study 2010, *The Lancet*, 380, 2224-2260, 10.1016/S0140-
862 6736(12)61766-8, 2012.
863
864 Lin, P., and Yu, J. Z.: Generation of Reactive Oxygen Species Mediated by Humic-like
865 Substances in Atmospheric Aerosols, *Environmental Science & Technology*, 45, 10362-10368,
866 10.1021/es2028229, 2011.
867 Lin, Y.-H., Zhang, Z., Docherty, K. S., Zhang, H., Budisulistiorini, S. H., Rubitschun, C. L.,
868 Shaw, S. L., Knipping, E. M., Edgerton, E. S., Kleindienst, T. E., Gold, A., and Surratt, J. D.:
869 Isoprene Epoxydiols as Precursors to Secondary Organic Aerosol Formation: Acid-Catalyzed
870 Reactive Uptake Studies with Authentic Compounds, *Environmental science & technology*, 46,
871 250-258, 10.1021/es202554c, 2012.
872 Lin, Y.-H., Arashiro, M., Martin, E., Chen, Y., Zhang, Z., Sexton, K. G., Gold, A., Jaspers, I.,
873 Fry, R. C., and Surratt, J. D.: Isoprene-Derived Secondary Organic Aerosol Induces the
874 Expression of Oxidative Stress Response Genes in Human Lung Cells, *Environmental Science &*
875 *Technology Letters*, 3, 250-254, 10.1021/acs.estlett.6b00151, 2016.
876 Lin, Y.-H., Arashiro, M., Clapp, P. W., Cui, T., Sexton, K. G., Vizuete, W., Gold, A., Jaspers, I.,
877 Fry, R. C., and Surratt, J. D.: Gene Expression Profiling in Human Lung Cells Exposed to
878 Isoprene-Derived Secondary Organic Aerosol, *Environmental Science & Technology*,
879 10.1021/acs.est.7b01967, 2017.
880 Lorentzen, R. J., Lesko, S. A., McDonald, K., and Ts'o, P. O. P.: <div
881 xmlns="http://www.w3.org/1999/xhtml">Toxicity of Metabolic
882 Benzo(a)pyrenediones to Cultured Cells and the Dependence upon Molecular
883 Oxygen</div>, *Cancer Research*, 39, 3194-3198, 1979.

884 Loza, C. L., Craven, J. S., Yee, L. D., Coggon, M. M., Schwantes, R. H., Shiraiwa, M., Zhang,
885 X., Schilling, K. A., Ng, N. L., Canagaratna, M. R., Ziemann, P. J., Flagan, R. C., and Seinfeld,
886 J. H.: Secondary organic aerosol yields of 12-carbon alkanes, *Atmos. Chem. Phys.*, 14, 1423-
887 1439, 10.5194/acp-14-1423-2014, 2014.

888 Lund, A. K., Doyle-Eisele, M., Lin, Y. H., Arashiro, M., Surratt, J. D., Holmes, T., Schilling, K.
889 A., Seinfeld, J. H., Rohr, A. C., Knipping, E. M., and McDonald, J. D.: The effects of alpha-
890 pinene versus toluene-derived secondary organic aerosol exposure on the expression of markers
891 associated with vascular disease, *Inhal. Toxicol.*, 25, 309-324, 10.3109/08958378.2013.782080,
892 2013.

893 Matsunaga, K., Klein, T. W., Friedman, H., and Yamamoto, Y.: Involvement of Nicotinic
894 Acetylcholine Receptors in Suppression of Antimicrobial Activity and Cytokine Responses of
895 Alveolar Macrophages to *Legionella pneumophila* Infection by Nicotine, *The
896 Journal of Immunology*, 167, 6518-6524, 10.4049/jimmunol.167.11.6518, 2001.

897 Mbawuike, I. N., and Herscowitz, H. B.: MH-S, a murine alveolar macrophage cell line:
898 morphological, cytochemical, and functional characteristics, *Journal of Leukocyte Biology*, 46,
899 119-127, 1989.

900 McDonald, J. D., Doyle-Eisele, M., Campen, M. J., Seagrave, J., Holmes, T., Lund, A., Surratt,
901 J. D., Seinfeld, J. H., Rohr, A. C., and Knipping, E. M.: Cardiopulmonary response to inhalation
902 of biogenic secondary organic aerosol, *Inhal. Toxicol.*, 22, 253-265,
903 10.3109/08958370903148114, 2010.

904 McDonald, J. D., Doyle-Eisele, M., Kracko, D., Lund, A., Surratt, J. D., Hersey, S. P., Seinfeld,
905 J. H., Rohr, A. C., and Knipping, E. M.: Cardiopulmonary response to inhalation of secondary
906 organic aerosol derived from gas-phase oxidation of toluene, *Inhal. Toxicol.*, 24, 689-697,
907 10.3109/08958378.2012.712164, 2012.

908 McWhinney, R. D., Zhou, S., and Abbatt, J. P. D.: Naphthalene SOA: redox activity and
909 naphthoquinone gas-particle partitioning, *Atmos. Chem. Phys.*, 13, 9731-9744, 10.5194/acp-13-
910 9731-2013, 2013.

911 Mohr, C., Huffman, J. A., Cubison, M. J., Aiken, A. C., Docherty, K. S., Kimmel, J. R., Ulbrich,
912 I. M., Hannigan, M., and Jimenez, J. L.: Characterization of Primary Organic Aerosol Emissions
913 from Meat Cooking, Trash Burning, and Motor Vehicles with High-Resolution Aerosol Mass
914 Spectrometry and Comparison with Ambient and Chamber Observations, *Environmental Science
915 & Technology*, 43, 2443-2449, 10.1021/es8011518, 2009.

916 Ng, N. L., Chhabra, P. S., Chan, A. W. H., Surratt, J. D., Kroll, J. H., Kwan, A. J., McCabe, D.
917 C., Wennberg, P. O., Sorooshian, A., Murphy, S. M., Dalleska, N. F., Flagan, R. C., and
918 Seinfeld, J. H.: Effect of NO_x level on secondary organic aerosol (SOA) formation from the
919 photooxidation of terpenes, *Atmos. Chem. Phys.*, 7, 5159-5174, 10.5194/acp-7-5159-2007,
920 2007a.

921 Ng, N. L., Kroll, J. H., Chan, A. W. H., Chhabra, P. S., Flagan, R. C., and Seinfeld, J. H.:
922 Secondary organic aerosol formation from m-xylene, toluene, and benzene, *Atmos. Chem. Phys.*,
923 7, 3909-3922, 10.5194/acp-7-3909-2007, 2007b.

924 Ng, N. L., Canagaratna, M. R., Zhang, Q., Jimenez, J. L., Tian, J., Ulbrich, I. M., Kroll, J. H.,
925 Docherty, K. S., Chhabra, P. S., Bahreini, R., Murphy, S. M., Seinfeld, J. H., Hildebrandt, L.,

926 Donahue, N. M., DeCarlo, P. F., Lanz, V. A., Prévôt, A. S. H., Dinar, E., Rudich, Y., and
927 Worsnop, D. R.: Organic aerosol components observed in Northern Hemispheric datasets from
928 Aerosol Mass Spectrometry, *Atmos. Chem. Phys.*, 10, 4625-4641, 10.5194/acp-10-4625-2010,
929 2010.

930 Ng, N. L., Canagaratna, M. R., Jimenez, J. L., Chhabra, P. S., Seinfeld, J. H., and Worsnop, D.
931 R.: Changes in organic aerosol composition with aging inferred from aerosol mass spectra,
932 *Atmos. Chem. Phys.*, 11, 6465-6474, 10.5194/acp-11-6465-2011, 2011.

933 Nguyen, T. B., Roach, P. J., Laskin, J., Laskin, A., and Nizkorodov, S. A.: Effect of humidity on
934 the composition of isoprene photooxidation secondary organic aerosol, *Atmos. Chem. Phys.*, 11,
935 6931-6944, 10.5194/acp-11-6931-2011, 2011.

936 Oberdörster, G., Ferin, J., Gelein, R., Soderholm, S. C., and Finkelstein, J.: Role of the alveolar
937 macrophage in lung injury: studies with ultrafine particles, *Environmental Health Perspectives*,
938 97, 193-199, 1992.

939 Oberdörster, G.: Lung Dosimetry: Pulmonary Clearance of Inhaled Particles, *Aerosol Sci.*
940 *Technol.*, 18, 279-289, 10.1080/02786829308959605, 1993.

941 Pan, Q., and Shimizu, I.: Imputation Variance Estimation by Multiple Imputation Method for the
942 National Hospital Discharge Survey, 2009.

943 Pardo, M., Shafer, M. M., Rudich, A., Schauer, J. J., and Rudich, Y.: Single Exposure to near
944 Roadway Particulate Matter Leads to Confined Inflammatory and Defense Responses: Possible
945 Role of Metals, *Environmental Science & Technology*, 49, 8777-8785, 10.1021/acs.est.5b01449,
946 2015.

947 Philip, M., Rowley, D. A., and Schreiber, H.: Inflammation as a tumor promoter in cancer
948 induction, *Seminars in Cancer Biology*, 14, 433-439,
949 <http://dx.doi.org/10.1016/j.semcan.2004.06.006>, 2004.

950 Piccot, S. D., Watson, J. J., and Jones, J. W.: A global inventory of volatile organic compound
951 emissions from anthropogenic sources, *Journal of Geophysical Research: Atmospheres*, 97,
952 9897-9912, 10.1029/92JD00682, 1992.

953 Platt, S. M., Haddad, I. E., Pieber, S. M., Huang, R. J., Zardini, A. A., Clairotte, M., Suarez-
954 Bertoia, R., Barmet, P., Pfaffenberger, L., Wolf, R., Slowik, J. G., Fuller, S. J., Kalberer, M.,
955 Chirico, R., Dommen, J., Astorga, C., Zimmermann, R., Marchand, N., Hellebust, S., Temime-
956 Roussel, B., Baltensperger, U., and Prévôt, A. S. H.: Two-stroke scooters are a dominant source
957 of air pollution in many cities, *Nature Communications*, 5, 3749, 10.1038/ncomms4749
958 <http://www.nature.com/articles/ncomms4749#supplementary-information>, 2014.

959 Pope, C. A., Burnett, R. T., Thun, M. J., Calle, E. E., Krewski, D., Ito, K., and Thurston, G. D.:
960 Lung cancer, cardiopulmonary mortality, and long-term exposure to fine particulate air pollution,
961 *Jama-Journal of the American Medical Association*, 287, 1132-1141, 10.1001/jama.287.9.1132,
962 2002.

963 Pope III, C. A., and Dockery, D. W.: Health effects of fine particulate air pollution: Lines that
964 connect, *Journal of the Air and Waste Management Association*, 56, 709-742, 2006.

965 Rattanavaraha, W., Rosen, E., Zhang, H., Li, Q., Pantong, K., and Kamens, R. M.: The reactive
966 oxidant potential of different types of aged atmospheric particles: An outdoor chamber study,
967 *Atmos. Environ.*, 45, 3848-3855, <http://dx.doi.org/10.1016/j.atmosenv.2011.04.002>, 2011.

968 Robinson, A. L., Donahue, N. M., Shrivastava, M. K., Weitkamp, E. A., Sage, A. M., Grieshop,
969 A. P., Lane, T. E., Pierce, J. R., and Pandis, S. N.: Rethinking Organic Aerosols: Semivolatile
970 Emissions and Photochemical Aging, *Science*, 315, 1259-1262, 10.1126/science.1133061, 2007.

971 Rogge, W. F., Hildemann, L. M., Mazurek, M. A., Cass, G. R., and Simoneit, B. R. T.: Sources
972 of fine organic aerosol. 1. Charbroilers and meat cooking operations, *Environmental Science &*
973 *Technology*, 25, 1112-1125, 10.1021/es00018a015, 1991.

974 Saffari, A., Hasheminassab, S., Wang, D., Shafer, M. M., Schauer, J. J., and Sioutas, C.: Impact
975 of primary and secondary organic sources on the oxidative potential of quasi-ultrafine particles
976 (PM0.25) at three contrasting locations in the Los Angeles Basin, *Atmos. Environ.*, 120, 286-
977 296, <http://dx.doi.org/10.1016/j.atmosenv.2015.09.022>, 2015.

978 Sankaran, K., and Herscowitz, H. B.: Phenotypic and functional heterogeneity of the murine
979 alveolar macrophage-derived cell line MH-S, *Journal of Leukocyte Biology*, 57, 562-568, 1995.

980 Spector, A. A., and Yorek, M. A.: Membrane lipid composition and cellular function, *Journal of*
981 *Lipid Research*, 26, 1015-1035, 1985.

982 Stirnweis, L., Marcolli, C., Dommen, J., Barmet, P., Frege, C., Platt, S. M., Bruns, E. A., Krapf,
983 M., Slowik, J. G., Wolf, R., Prévôt, A. S. H., El-Haddad, I., and Baltensperger, U.: α -Pinene
984 secondary organic aerosol yields increase at higher relative humidity and low NO_x conditions,
985 *Atmos. Chem. Phys. Discuss.*, 2016, 1-41, 10.5194/acp-2016-717, 2016.

986 Surratt, J. D., Chan, A. W. H., Eddingsaas, N. C., Chan, M., Loza, C. L., Kwan, A. J., Hersey, S.
987 P., Flagan, R. C., Wennberg, P. O., and Seinfeld, J. H.: Reactive intermediates revealed in
988 secondary organic aerosol formation from isoprene, *Proceedings of the National Academy of*
989 *Sciences*, 107, 6640-6645, 10.1073/pnas.0911114107, 2010.

990 Tao, F., Gonzalez-Flecha, B., and Kobzik, L.: Reactive oxygen species in pulmonary
991 inflammation by ambient particulates, *Free Radical Biology and Medicine*, 35, 327-340,
992 [http://dx.doi.org/10.1016/S0891-5849\(03\)00280-6](http://dx.doi.org/10.1016/S0891-5849(03)00280-6), 2003.

993 Tasoglou, A., and Pandis, S. N.: Formation and chemical aging of secondary organic aerosol
994 during the β -caryophyllene oxidation, *Atmos. Chem. Phys.*, 15, 6035-6046, 10.5194/acp-15-
995 6035-2015, 2015.

996 Terada, H.: Uncouplers of oxidative phosphorylation, *Environmental Health Perspectives*, 87,
997 213-218, 1990.

998 Tuet, W. Y., Fok, S., Verma, V., Tagle Rodriguez, M. S., Grosberg, A., Champion, J. A., and
999 Ng, N. L.: Dose-dependent intracellular reactive oxygen and nitrogen species (ROS/RNS)
1000 production from particulate matter exposure: comparison to oxidative potential and chemical
1001 composition, *Atmos. Environ.*, 144, 335-344, <http://dx.doi.org/10.1016/j.atmosenv.2016.09.005>,
1002 2016.

1003 Tuet, W. Y., Chen, Y., Xu, L., Fok, S., Gao, D., Weber, R. J., and Ng, N. L.: Chemical oxidative
1004 potential of secondary organic aerosol (SOA) generated from the photooxidation of biogenic and

1005 anthropogenic volatile organic compounds, *Atmos. Chem. Phys.*, 17, 839-853, 10.5194/acp-17-
1006 839-2017, 2017.

1007 Van Krevelen, D.: Graphical-statistical method for the study of structure and reaction processes
1008 of coal, *Fuel*, 29, 269-284, 1950.

1009 Verma, V., Shafer, M. M., Schauer, J. J., and Sioutas, C.: Contribution of transition metals in the
1010 reactive oxygen species activity of PM emissions from retrofitted heavy-duty vehicles, *Atmos.*
1011 *Environ.*, 44, 5165-5173, 10.1016/j.atmosenv.2010.08.052, 2010.

1012 Verma, V., Rico-Martinez, R., Kotra, N., King, L., Liu, J. M., Snell, T. W., and Weber, R. J.:
1013 Contribution of Water-Soluble and Insoluble Components and Their Hydrophobic/Hydrophilic
1014 Subfractions to the Reactive Oxygen Species-Generating Potential of Fine Ambient Aerosols,
1015 *Environmental Science & Technology*, 46, 11384-11392, 10.1021/es302484r, 2012.

1016 Verma, V., Fang, T., Xu, L., Peltier, R. E., Russell, A. G., Ng, N. L., and Weber, R. J.: Organic
1017 Aerosols Associated with the Generation of Reactive Oxygen Species (ROS) by Water-Soluble
1018 PM2.5, *Environmental Science & Technology*, 49, 4646-4656, 10.1021/es505577w, 2015a.

1019 Verma, V., Wang, Y., El-Afifi, R., Fang, T., Rowland, J., Russell, A. G., and Weber, R. J.:
1020 Fractionating ambient humic-like substances (HULIS) for their reactive oxygen species activity
1021 – Assessing the importance of quinones and atmospheric aging, *Atmos. Environ.*, 120, 351-359,
1022 <http://dx.doi.org/10.1016/j.atmosenv.2015.09.010>, 2015b.

1023 Vivanco, M. G., and Santiago, M.: Secondary Organic Aerosol Formation from the Oxidation of
1024 a Mixture of Organic Gases in a Chamber, *Air Quality*, Ashok Kumar (Ed.), InTech, DOI:
1025 10.5772/9761. Available from: <http://www.intechopen.com/books/air-quality/secondary-organic-aerosols-experiments-in-an-outdoor-chamber->, 2010.

1027 Wang, H., Czura, C., and Tracey, K.: Tumor necrosis factor, *The cytokine handbook*, 4, 837-860,
1028 2003.

1029 Wen, Y., Gu, J., Chakrabarti, S. K., Aylor, K., Marshall, J., Takahashi, Y., Yoshimoto, T., and
1030 Nadler, J. L.: The Role of 12/15-Lipoxygenase in the Expression of Interleukin-6 and Tumor
1031 Necrosis Factor- α in Macrophages, *Endocrinology*, 148, 1313-1322, 10.1210/en.2006-0665,
1032 2007.

1033 Wiseman, H., and Halliwell, B.: Damage to DNA by reactive oxygen and nitrogen species: role
1034 in inflammatory disease and progression to cancer, *Biochem. J.*, 313, 17-29, 1996.

1035 Witkamp, R., and Monshouwer, M.: Signal transduction in inflammatory processes, current and
1036 future therapeutic targets: A mini review, *Veterinary Quarterly*, 22, 11-16,
1037 10.1080/01652176.2000.9695016, 2000.

1038 Wong, J. P. S., Lee, A. K. Y., and Abbatt, J. P. D.: Impacts of Sulfate Seed Acidity and Water
1039 Content on Isoprene Secondary Organic Aerosol Formation, *Environmental Science &*
1040 *Technology*, 49, 13215-13221, 10.1021/acs.est.5b02686, 2015.

1041 Xu, L., Kollman, M. S., Song, C., Shilling, J. E., and Ng, N. L.: Effects of NO_x on the Volatility
1042 of Secondary Organic Aerosol from Isoprene Photooxidation, *Environmental Science &*
1043 *Technology*, 48, 2253-2262, 10.1021/es404842g, 2014.

1044 Xu, L., Guo, H., Boyd, C. M., Klein, M., Bougiatioti, A., Cerully, K. M., Hite, J. R., Isaacman-
1045 VanWertz, G., Kreisberg, N. M., Knote, C., Olson, K., Koss, A., Goldstein, A. H., Hering, S. V.,

1046 de Gouw, J., Baumann, K., Lee, S.-H., Nenes, A., Weber, R. J., and Ng, N. L.: Effects of
1047 anthropogenic emissions on aerosol formation from isoprene and monoterpenes in the
1048 southeastern United States, *Proceedings of the National Academy of Sciences*, 112, 37-42,
1049 10.1073/pnas.1417609112, 2015.

1050 Zhang, Q., Jimenez, J. L., Canagaratna, M. R., Allan, J. D., Coe, H., Ulbrich, I., Alfarra, M. R.,
1051 Takami, A., Middlebrook, A. M., Sun, Y. L., Dzepina, K., Dunlea, E., Docherty, K., DeCarlo, P.
1052 F., Salcedo, D., Onasch, T., Jayne, J. T., Miyoshi, T., Shimono, A., Hatakeyama, S., Takegawa,
1053 N., Kondo, Y., Schneider, J., Drewnick, F., Borrmann, S., Weimer, S., Demerjian, K., Williams,
1054 P., Bower, K., Bahreini, R., Cottrell, L., Griffin, R. J., Rautiainen, J., Sun, J. Y., Zhang, Y. M.,
1055 and Worsnop, D. R.: Ubiquity and dominance of oxygenated species in organic aerosols in
1056 anthropogenically-influenced Northern Hemisphere midlatitudes, *Geophysical Research Letters*,
1057 34, n/a-n/a, 10.1029/2007GL029979, 2007.

1058